

Thermal Modelling of Water-Based Floor Heating Systems

- supply temperature optimisation and self-regulating effects

HENRIK KARLSSON

Department of Civil and Environmental Engineering
CHALMERS UNIVERSITY OF TECHNOLOGY
Göteborg, Sweden 2010

Thermal Modelling of Water-Based Floor Heating Systems
- supply temperature optimisation and self-regulating effects

HENRIK KARLSSON

ISBN 978-91-7385-369-9

© HENRIK KARLSSON, 2010.

Doktorsavhandlingar vid Chalmers tekniska högskola

Ny serie nr: 3050

ISSN: 0346-718X

Department of Civil and Environmental Engineering

Division of Building Technology

Chalmers University of Technology

SE-412 96 Göteborg

Sweden

Telephone + 46 (0)31-772 1000

<http://www.chalmers.se>

Chalmers Reproservice

Göteborg, Sweden 2010

HENRIK KARLSSON

Department of Civil and Environmental Engineering
Division of Building Technology
Chalmers University of Technology

Abstract

Low temperature water-based concrete embedded floor heating systems are studied. The utilisation of low quality heat sources is facilitated by low temperature heating. Theoretical models which describe the transient thermal floor heating operation constitute the basis for the analysis. The combination of building, floor heating element, heat gains and control system is described by a set of theoretical models. In particular, a numerical floor heating element model is developed and verified by comparison with results from heat transfer software and published experimental results.

A model based predictive control method is applied in order to find an optimised supply fluid temperature. The aim is to keep the upcoming operative temperature within a comfort interval and at the same time constrain the supply heat flux within practical limits. A discrete transient response factor method is utilised by a numerical optimisation algorithm that iteratively finds an optimised solution. The response factor method describes the relation between a piecewise constant supply heat flux and the succeeding shift in indoor temperature. The stability of the system has been studied; the initial delay time caused by the time needed for a heat front to conduct from the depth of the embedded circuit towards the interior sets a limit for the applied period time in the discrete response method. The predictive optimisation method has been applied in a realistic case where the operative temperature is successfully kept within the comfort interval.

The self-regulation ability due to a thermal perturbation in the case of feed-forward controlled supply temperature is studied separately. Such system counteracts any non-periodic thermal perturbation by shifting the supplied heat flux in the opposite direction. The outcome is a more even indoor temperature and enhanced utilisation of heat gains. Transient response functions which quantify the involved thermal processes are derived by the developed model. It has been shown that the transient shift in supplied heat flux is given by two coupled processes. The first process is related to the propagation of heat towards the position of the embedded circuit due to the perturbation. The second process is related to the heat exchange along the embedded circuit due to the excitation of the supply temperature. The demand of an unchanged supply temperature connects the two processes (i.e. from the feed-forward supply temperature control). The self-regulation utilisation factor is defined as the ratio between the accumulated shift in supply heat flux and the energy content of a finite thermal perturbation. Buildings with small heat losses in combination with a high equivalent thermal conductance from the supply of the pipe circuit towards the interior yields a high self-regulation utilisation factor. Hence, self-regulation is an integrated phenomenon which depends on both the design of the floor heating element and the building.

Keywords: Floor heating, low temperature heating, self-regulation, predictive control.

List of publications

This thesis consists of papers presented at international peer reviewed conferences and papers accepted in, or submitted to, scientific journals. The term “*building integrated heating*” is used in Paper I, II and III. In the later papers the terminology is adapted according to the *EN 15377* standard (CEN, 2008). Hence, in Paper IV, V, VI and VII the corresponding term is changed into “*embedded surface heating*”.

Appended papers

- I. Karlsson, H. and Hagentoft, C.-E. (2005). Modelling of Long Wave Radiation Exchange in Enclosures with Building Integrated Heating, *Proceedings of the 7th Symposium on Building Physics in the Nordic Countries*, Reykjavík, Iceland.
- II. Karlsson, H. (2007). An innovative floor heating application - Transfer of excess heat between two building zones. *Proceedings of the 10th International Building performance Simulation (IBPSA) Conference*, 148-155. Beijing, China.
- III. Karlsson, H. (2008). Self-Regulating Floor Heating Systems in Low Energy Buildings. *Proceedings of the 8th Symposium on Buildings Physics in the Nordic Countries*, 519-526. Copenhagen, Denmark.
- IV. Karlsson, H. (2010). Embedded water-based surface heating, Part 1: Hybrid three-dimensional numerical model. *Journal of Building Physics*, 33(4): 357-392.
- V. Karlsson, H. (2011). Embedded water-based surface heating, Part 2: Experimental validation. *Journal of Building Physics*, 34(4). (In press)
- VI. Karlsson, H. and Hagentoft, C.-E. (2010). Self-regulated water-based floor heating analysed by a response factor method. Submitted to *Building and Environment*.
- VII. Karlsson, H. and Hagentoft, C.-E. (2010). Application of model based predictive control for water-based floor heating in low energy residential buildings. Submitted to *Building and Environment*.

Other publications related to the work in this thesis

Hagentoft, C.-E. and Karlsson, H. (2007). *Golvvärme – Något för framtiden!*. Rapport 2007:14. Civil and Environmental Engineering, Chalmers University of Technology, Göteborg, Sweden.

Karlsson, H. (2006). *Thermal system analysis of embedded building integrated heating – numerical model and validation of hydronic floor heating systems*. Thesis for the degree of licentiate of engineering. Chalmers University of Technology, Göteborg, Sweden.

Hagentoft, C.-E., Karlsson, H. and Sasic Kalagasidis, A. (2008). Floor heating in buildings with small energy demand for heating – Feasibilities for the control of the internal temperature using heating. *Proceedings of the Buildings Physics Symposium in honour of Professor Hugo L.S.C. Hens*, 85-89. Leuven, Belgium.

Preface

The work presented in this thesis has been carried out at the Division of Building Technology/ Building Physics Research group, Department of Civil and Environmental Engineering at Chalmers University of Technology. The research project is financially supported by the Swedish Energy Agency and the Construction Industry Organisation for Research and Development in Sweden (SBUF-FoU Väst), the support is gratefully appreciated. I would like to thank the members of the project reference group for your interest in the work and for your good advises.

My supervisors during this work have been Professor Carl-Eric Hagentoft and Associate Professor Angela Sasic Kalagasidis. I would like to thank for the deep thoughtfulness you both have shown me. To my colleagues at the division of Building Technology - thank you all for the support and the friendly atmosphere that you all contribute to.

Henrik Karlsson

Göteborg, February 2010

Contents

Abstract	i
List of publications	iii
Preface	v
1 Introduction	1
1.1 Background	1
1.2 Hypothesis	4
1.3 Limits and assumptions	5
1.4 Method	6
2 Calculation methods	7
2.1 Development of embedded surface heating model in Simulink	7
2.2 Verification of the Simulink model	11
2.3 Simplified lumped 2-node model	16
3 Determination of the supply fluid temperature	19
3.1 Optimised supply fluid temperature	19
3.2 Simplified methods in order to calculate the heat supply	24
4 Self-regulation ability of water-based floor heating	29
4.1 Introduction	29
4.2 Transient response analyse	29
4.3 The consequence on the indoor temperature due to self-regulation	32
4.4 Self-regulation due to periodical perturbances	34
5 Conclusions	35
6 Further studies	37
7 References	39
Appendix	
Appended Papers I-VII	

1 Introduction

1.1 Background

The estimated final energy use for heating and hot water (per square meter heated floor area) in the Swedish building stock shows a decreasing trend, see Figure 1. The average one- and two-dwelling buildings have a final energy use in the range of 125 kWh/m²/year and multi-dwelling buildings 150 kWh/m²/year during 2007. Beside the effect on the final energy use due to conversion from oil to heat pumps, the decreasing trend is due to energy efficiency measures in the building stock. The heat demand has decreased through improvements of windows, building envelopes, ventilation system, efficient hot water use and adjustment of heating systems and so on. The total energy supply in the Swedish energy system 2008, was 612 TWh (Swedish Energy Agency, 2009A). The total final energy use (397 TWh excluding conversion and distribution losses) is mainly supplied to the industry, the transport and the dwelling- and service sector. The dwelling and service sector (141 TWh year 2008) stands for approximately 36% of the final energy use in the Swedish energy system. The estimated temperature corrected final energy use for space heating and hot water purpose in the dwelling and service sector 2007, was 78.2 TWh (Swedish Energy Agency, 2009B).

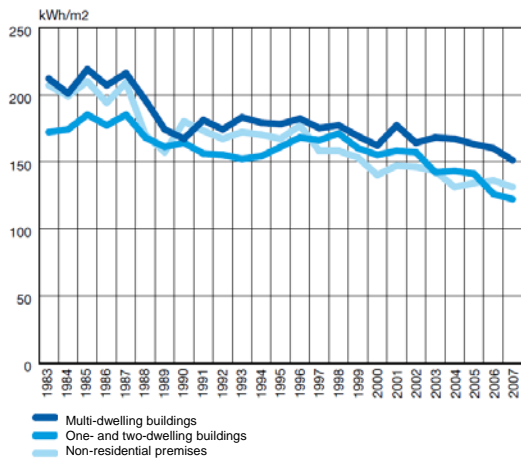


Figure 1 Final energy use for heating and hot water per heated floor area unit (not temperature corrected). Swedish Energy Agency (2009B and 2009C).

The energy use in the dwelling sector is expected to decrease in the future due to stricter energy and environmental policies. The Swedish energy policy regarding energy use in the dwelling and service sectors was re-formulated in 2006:

“The final energy use (per heated floor area unit) should decrease. The decrease should be 20% by the year of 2020 and 50% by the year of 2050 in comparison to the final use in 1995. The dependency on fossil fuels in the dwelling sector should be broken by the year of 2020 while renewable energy is continuously increasing.”

The EU-27 countries are dependent on fossil fuels. Fossil fuels constituted 79% of the energy supply in 2006; approximately 37% of the final energy use is related to the dwelling and service sector (Eurostat, 2009). Energy related green house gas emissions stands for 80% of all emissions in EU-27; today climate mitigation goals constitute the core aim of the EU energy policy. Energy efficiency measures in the dwelling sector are important when it comes to climate change mitigation and

reduction of imported fossil fuels dependency. The member states in the EU have agreed on the next edition of the directive in the energy performance of buildings (EU-Directive 2002/91/EC) in November 2009 (European Parliament, 2009). The intention is to improve the existing building stock and to significantly reduce the heat demand for new buildings:

“By the end of 2020 EU Member States must ensure that all newly-constructed buildings have a “very high energy performance”, And their energy needs must be covered to a very significant extent from renewable sources, including energy produced on-site or nearby.”

The choice of heating system at building level plays a major role in primary energy use since it determines the type of energy supply chains that can be used (Joelsson, 2008). Heat sources of low energy quality are an appealing alternative regarding space heating in dwellings. Surplus heat or low temperature geothermal heat are examples of low quality energy sources. The use of surplus heat leads to a reduced need for primary resources in the energy system as a whole. Utilisation of low quality heat sources are facilitated by the fact that the heat supply system within the building operates at a low temperature.

Low temperature heating means that the required temperature of the heat carrier is low. The exact temperature level depends on the considered technology (i.e. heat supply system) and on the present heat demand of the building. The temperature range is from a few degrees, to approximately 15 degrees, above comfortable room temperature. The purpose of shifting to low temperature heating technology is not necessarily to decrease the heat demand of the building but it is beneficial for the energy system as whole since high quality energy sources becomes available for other purposes (Persson, 2000). Efficient use of the available energy sources is a key parameter towards a sustainable energy system.

It is essential to decrease the return temperature level from the substations in a district heating system in order to improve the overall efficiency of the system. A decreased temperature level yields a reduction of distribution heat losses. The efficiency of heat generation plants, heat pumps and solar collectors benefits from a reduced temperature level in the district heating system. Furthermore, the ability to utilise surplus heat as a useful heat source in the district heating system increases. The required increase in pump power is small if a new building can be connected to the return pipe instead of the primary pipe of an existing district heating system. Such substation connection is possible if the connected building can make use of a lower temperature. As a result, the net return temperature from the substation becomes even lower. It is appealing to build secondary district heating systems which operate at low temperatures for clusters of low energy buildings (Persson, 2000).

The heat pump moves heat from a cold source (i.e. ground, water, outdoor air or exhaust air) to a higher temperature level by using mechanical work (i.e. electric energy). The coefficient of performance (COP) is the ratio between the useful heat movement and the work input required to run the machine. According to the Carnot efficiency, the performance of the heat pump benefits from the fact that the heat supply system is designed with a low temperature. As a brief example, heat pumps for single family houses have COP in the range of 3.5 if the temperature lift is from 0°C to 55°C while the COP increases to 4.9 for the same heat pump if a low temperature system is applied (0°C to 35°C).

Low temperature heating is mainly accomplished by applying large internal heat transferring areas such as floors, ceiling and walls (Persson, 2000). *Embedded surface heating* is the generic name of a heat supply system that is integrated within the building structure; according to the European standard EN 15377 (CEN, 2008). Through the history, the building structure has been utilised for space heating purpose during many thousands of years; Chinese *Kang*, Korean *Ondol* and Roman & Greek *Hypocaust* systems are historical examples of embedded surface heating (Bean et al., 2010). Water-based floor heating is a typical example of modern embedded surface heating, see Figure 2. Heat is supplied to the building structure by means of pipes or ducts embedded in a casted layer of concrete, screed or similar building material. The systems can also be fitted within wooden constructions; heat conduction plates, typically of aluminium, are in this case mounted close to the pipe circuit in order to facilitate lateral heat conduction. The embedded pipe/duct system in union with the adjoining building structure function as a large heat exchanger. The element is at the same time part of the building envelope where heat is conducted from the inside towards the outside.



Figure 2 Illustration of a floor heating construction. On the left-hand side a concrete embedded system and on the right-hand side a light weight system with heat conduction plates fitted in a wooden joist. (By courtesy of Uponor)

The increased temperature at the depth of the pipe circuit induces an upward heat flux which corresponds to the useful fraction of the net supply heat flux; hence, the floor surface becomes warmer. The useful fraction of the supply heat flux equals the heat demand of the building if no other heating systems operate in the building. One disadvantage with floor heating is that there also exists an additional heat flux from the depth of the pipe circuit towards the ground or to the apartment below. This additional heat loss is due to the fact that heat is supplied within the building envelope; partly outside the interior space. The ratio between the upward heat flux and the supply heat flux is given by the insulation efficiency η (Roots et al., 2005). The insulation efficiency depends mainly on the thickness of the underlying thermal insulation towards the ground and the thermal resistance of the floor covering material. The practical meaning is that thicker thermal ground insulation must be applied in the case of floor heating in comparison to an ideal heating system if the supply heat flux should remain constant. Hence, at least 250mm thermal insulation towards the ground and the use of floor material with low thermal resistance (i.e. avoidance of thick wooden floors etc.) is given as a general recommendation (Swedish Energy Agency et al.).

A concrete floor slab, which embeds the pipe circuit, comprises a significant thermal mass that leads to a delay time between the heat supply and the response in indoor temperature. A drawback with conventional control techniques is their inability to compensate for the delay time and to adapt to changing dynamics (Chen, 2001). The thermal mass of the floor heating system is not necessarily a negative thing; the thermal mass of buildings can be utilised as short-time thermal storage in a

district heating system (Wigbels et al., 2005). The storage yields a heat buffer which can be useful in order to level out the heat generation in the district heating system. The storage effect is higher for thermally heavy heat supply systems such as concrete embedded floor heating; heat can be stored within the slab without a subsequent increase of the indoor temperature.

The temperature decrease from the supply towards the return end of the floor heating pipe circuit is lower in comparison to a hydronic radiator system. Large temperature differences along the circuit would yield an uneven floor surface temperature which is uncomfortable. Hence, for the same supply heat flux the fluid flow rate is higher in the floor heating case which yields an increased auxiliary heat loss for circulation pumps (Olesen et al., 2009).

A significant share of the investment cost for floor heating is allocated to the cost for the control system; in particular room control (i.e. room thermostats for each pipe circuit) can be estimated to 25-40% of the total investment cost for concrete embedded floor heating according to two manufacturers. Concrete or screed embedded systems are significantly cheaper than systems for light-weight wooden construction. These light systems consist of more components (i.e. heat conduction plates and particle boards with immersed tracks for the pipe loops).

In the case of passive houses, the additional investment cost for decreasing the heat demand is to some extent compensated by cost reductions due to a simplified heat supply system. The heat demand is reduced to a minimum in the passive house design principle. Swedish passive houses are mainly equipped with an air-based heating system which utilises the supply air flow as heat carrier. According to the simulations (Jansson, 2008), the supply air temperature may exceed the requirement of maximally +52°C during winter conditions, air exchange rate of 0.5h^{-1} and a set point temperature at +22°C. Overall, few examples of low energy buildings fitted with floor heating are documented in Sweden. Beiron et al. (2007) describes experiences and measurements from the operation of a well insulated multi-dwelling building fitted with floor heating.

There is an interest in exploring the transient operation of the floor heating system fitted in well insulated residential buildings. Such combination yields very low supply temperatures. The possibility to simplify the system design and the control without jeopardising thermal comfort is also of interest; such simplification would reduce the investment cost and facilitate utilisation of heat sources of low energy quality.

1.2 Hypothesis

Space heating in residential buildings with a low heat demand is achievable by means of low temperature water-based floor heating. Acceptable thermal comfort is attainable through a prescribed supply water temperature and the self-regulation ability although active thermal control at room level is rejected. The optimal supply fluid temperature can show small variations in amplitude and time. Hence, simple control strategies are possible without jeopardising thermal comfort.

1.3 Limits and assumptions

The combination of a well insulated residential building fitted with low temperature water-based floor heating is studied. The floor heating pipes are embedded within a concrete slab. One and two-dwelling buildings with a concrete slab on ground foundation are considered. The purpose of the floor heating system is to provide space heating during the heating system. The building itself is the boundary of the studied system; hence, the energy system outside the building is not considered explicitly, see Figure 3. The transient thermal system operation is considered through the use of theoretical models.

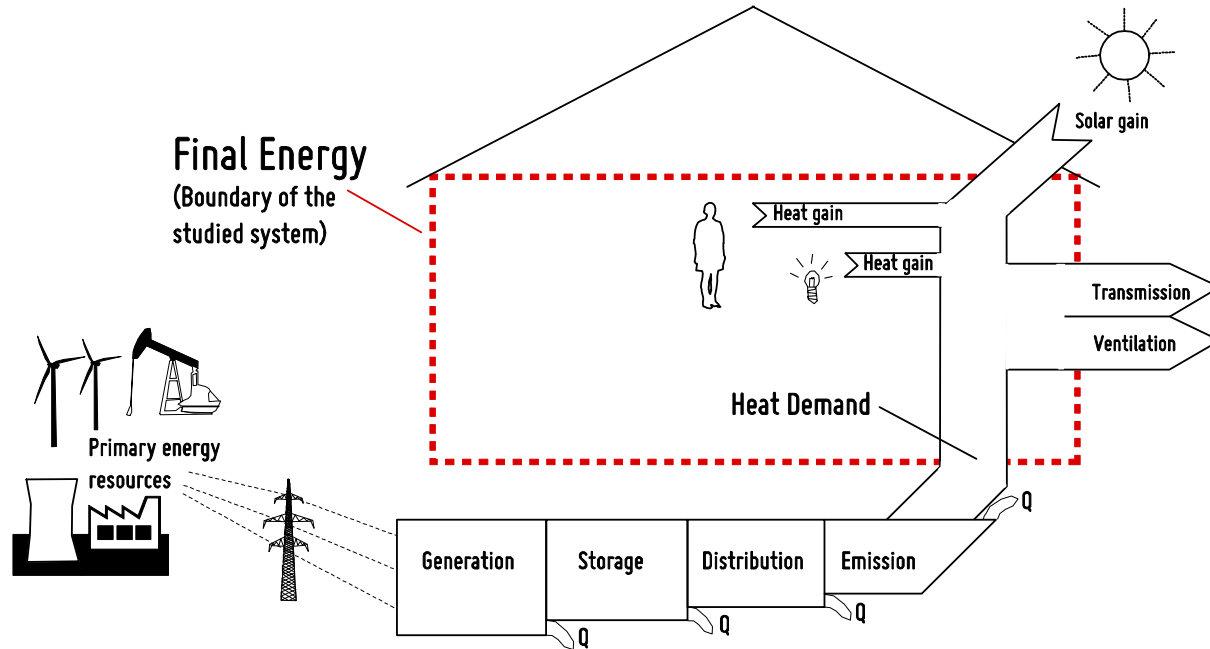


Figure 3 Illustration of energy supply chains and the boundaries of the study.

Within the system borders the considered system is affected by internal heat gains through heat emission from persons and their activities. These heat gains are predefined in amplitude and time according to the general behaviour. Incoming solar radiation is assumed to incident evenly on the entire floor surface followed by a diffuse reflection. The general theoretical model treats un-linear heat convection and heat radiation; however, in a part of the analysis a linear assumption is implemented in the theoretical model. The building is considered to be unfurnished.

Thermal comfort is estimated by the simplified operative temperature (i.e. the equal weight of the average surface temperature and the indoor air temperature). A well-mixed indoor air volume is assumed. The fluid temperature distribution along the embedded pipe is assumed as quasi steady state. The embedded pipe circuit is considered only through its heat exchange capability. The fluid flow rate and either supply temperature or supply heat flux, depending on the control method, are assumed ideally controlled. The hydraulic condition for the embedded pipe system is not explicitly accounted for. However, the fluid flow rate is constrained within limits which yields total pressure losses which corresponds to rules of thumb (i.e. maximum 20-25 kPa). Heat generated by the operation of the circulation pump is not accounted for.

The thesis does not generate a set of general guidelines for the design of the floor heating system (i.e. centre-to-centre distance, pipe mounting height, fluid flow rate, slab thickness, floor covering material etc.) or the building design (i.e. U-values or ventilation method).

1.4 Method

Theoretical models which describe the overall transient thermal floor heating operation constitute the basis for the analysis given in this thesis. The considered combination of building, floor heating element, heat gains and control system is described by set of theoretical models which together form a dynamic thermal system which is implanted in the Simulink software which works on top of the Matlab software. In detail, the general transient heat conduction problem within the floor slab is numerically solved by an explicit control volume method. The entire dynamic thermal system is simultaneously solved by the inbuilt numerical solver (i.e. by Simulink). The numerical model is hereafter referred to as the Simulink model.

The structure of the developed Simulink model is compatible with the pre-defined structure given by the International Building Physics Toolbox in Simulink (Weitzmann et al., 2003). The Simulink model is verified by comparison with validated heat transfer software and by comparison with published results from measurements of a concrete embedded floor heating system.

Superposition technique is applied in order to identify two elementary sub-processes which together describe the self-regulation effect. The clarification of the self-regulation phenomena is given through the use of a response factor method. The transient behaviour of the two sub-processes is derived from a step-change excitation of each sub-system which is numerically calculated by the Simulink model. Hence, the results obtained from the Simulink model is the basis for the applied response factor method.

The response factor method is also applied in order to describe the relation between the supply heat flux and the subsequent time-dependent indoor temperature response. The elementary pulse-response function is the basis for the control methods which are given in this thesis. A model based predictive control method (Garcia et al., 1989) is applied in order to optimise the control of the floor heating system. A numerical optimisation routine (i.e. the *fmincon* Matlab function) calculates iteratively the upcoming constrained supply heat flux which minimises the deviation between the indoor temperature and a given comfort interval. A simplified lumped 2-node model is considered as an alternative to the Simulink model in the analysis of control methods.

A description of a reference building equipped with water-based floor heating is appended. The reference building is frequently used in Paper III, VI and VII.

2 Calculation methods

Section 2.1 and 2.2 gives a brief summary of the developed theoretical models and its verification. These sections are based on Paper I, III and IV. Section 2.3 describes a simplified lumped model which is applied in Paper VII.

2.1 Development of embedded surface heating model in Simulink

The development of a numerical model that assesses the transient operation of embedded water-based constitutes an important part of the work presented in this thesis. The aim is to calculate the resulting indoor thermal conditions which occur due to a given design of the building including the embedded surface heating system. Relevant design parameters associated with the embedded surface heating system should be included as well as the control algorithm of the system. Water-based embedded surface heating systems are integrated in the structure of the building and the operation is very much dependent on the dynamic situation within the building. Figure 4 illustrate some of the dynamic interactions which affect the embedded system operation from a thermal point of view.

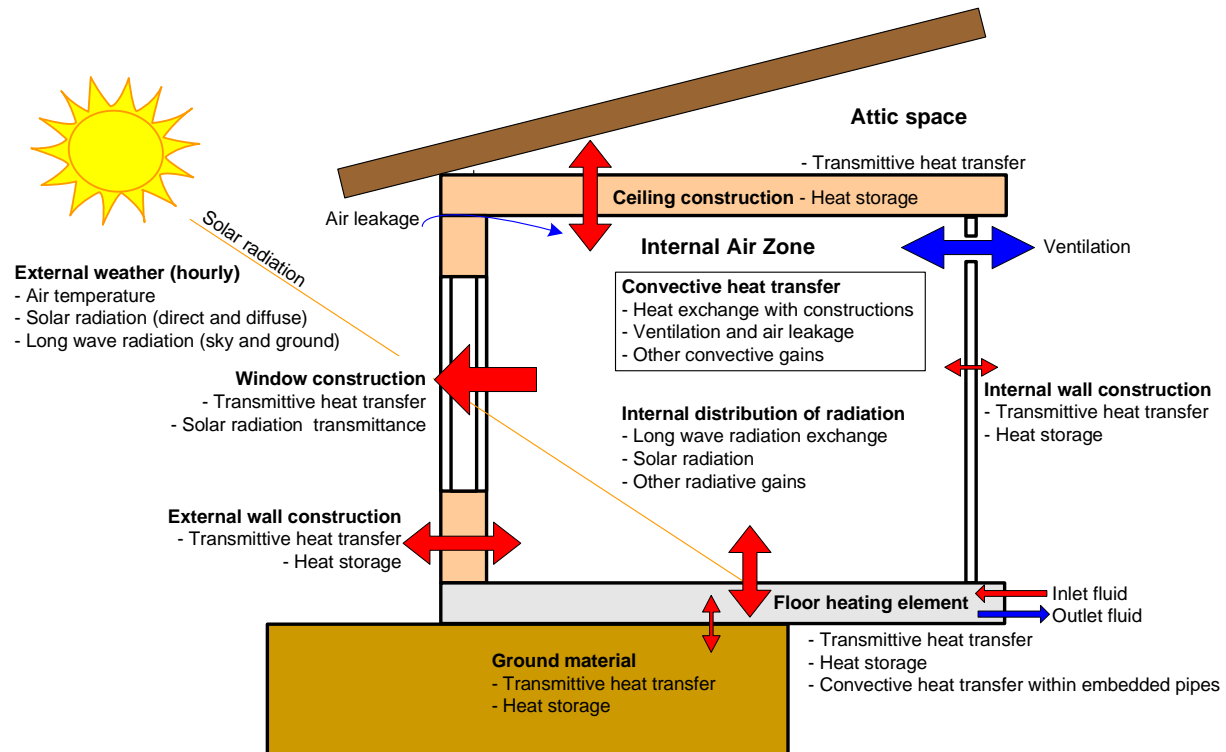


Figure 4 Illustration of the dynamic operation condition for the embedded surface heating system.

The International Building Physics Toolbox in Simulink (IBPT) and the HAM-Tools library (Sasic Kalagasis, 2004) are the starting point in the implementation of an embedded surface heating model. The software consists of several separate calculation procedures (tools), each representing certain building components or systems. By using the system of well defined data signals, tools can be combined in a more complex calculating procedure, leading to a prototype of a building as a system. Figure 5 illustrates the main categories of tools defined by IBPT; the intricate system of data signals which connect the tools with each other is not given. The entire Simulink model has the ability to perform a general thermal system analysis where the transient operation of the embedded surface heating system is assessed jointly with all relevant systems. The resulting indoor air

temperature, surface temperatures for the whole set of subsurfaces within the enclosure and the supply heat flux to the embedded system over time are the outputs from a calculation.

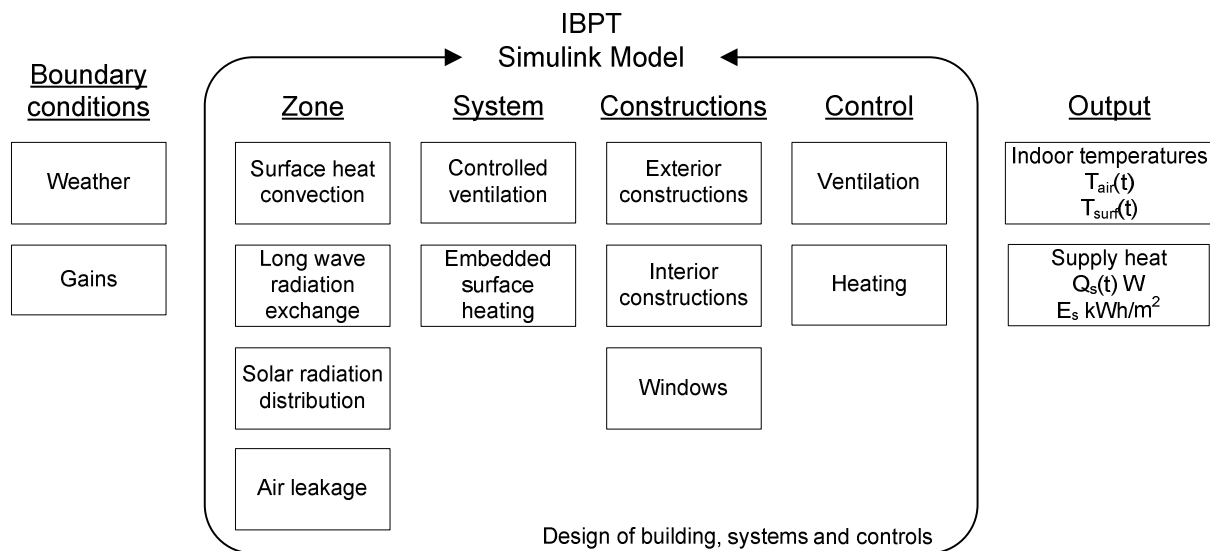


Figure 5 Illustration of the main components in the modular Simulink tool grouped according to IBPT.

The efforts in model improvement and development have been focusing on:

- Implementing an increased internal space discretisation of internal surfaces.
- Implementing a comprehensive long wave radiation exchange model between internal subsurfaces including methods for pre-calculation of view factors.
- Implementing two-dimensional heat conduction (explicit control volume method) in the embedded surface heating element and a pipe inclusion method in order to model the thermal interaction between the pipe circuit and the embedding material
- Implementing a model which describes the longitudinal heat convection due to the circulation of fluid in the embedded pipe circuit

The embedded surface heating element is subdivided in a number of smaller room sub surfaces, see Figure 6. In this manner, a spatial grid is established where the pipe circuits can be positioned. Thus, the spatial grid is determined by the desired pipe circuit pattern. The total length of the pipe circuit is subdivided in the same manner. The result is a sequence of pipe segments, see Figure 6 and Figure 7. For each subsurface/pipe segment, the underlying material volume is represented by a two-dimensional transversal section plane, see Figure 6. All section planes are perpendicular to the pipe direction and bounded by interior and exterior boundaries, all other boundaries are adiabatic. The section plane is built up by an arbitrary number of material layers. This means that the model comprises several important design parameters which together determine the heat exchange capability of the element: centre-to-centre distance, pipe mounting height, pipe circuit pattern, slab thickness, floor covering material, floor thickness and the thermal ground insulation.

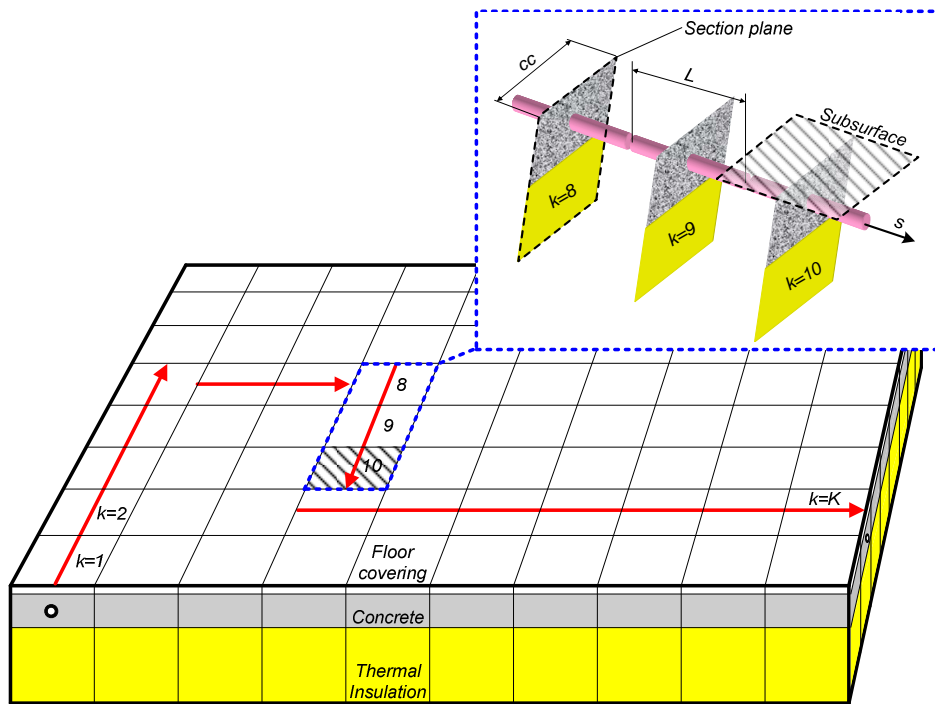


Figure 6 Sketch illustrating the spatial discretisation of a single embedded surface heating element, pointers designate the horizontal projection of the hydronic pipe position and the fluid motion. The inset displays three serially coupled section planes.

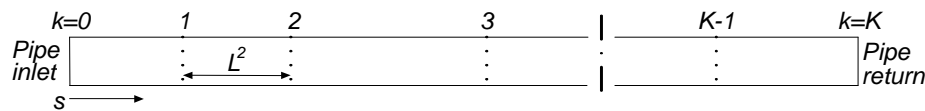


Figure 7 Longitudinal discretisation of pipe circuit into pipe segments. Index k denotes the fluid motion from inlet ($k=0$) to return ($k=K$).

The transient heat transfer in the embedded element is solved by an explicit control volume method. The pipe is fictitiously projected at the corner between four control volumes, called pipe inclusion control volumes. Thus, each segment of the pipe is divided in four quadrants, see Figure 8. Each pipe segment is thermally coupled to the corresponding section plane through the pipe quadrants. Hence, heat source terms are implemented in the calculation scheme at each pipe inclusion node. The transversal heat fluxes (i.e. the heat source terms) are determined by the temperature potential and the thermal resistance between the fluid and the pipe inclusion node (i.e. the sum of surface heat transfer resistance at the inner pipe wall surface, the pipe wall resistance and the resistance in the embedding material between the pipe and the inclusion node). The heat exchange is also longitudinally distributed along the embedded pipe circuit. The longitudinal fluid temperature distribution (from inlet to return) consists of a step-wise sequence of all pipe segment solutions which are calculated by applying local quasi steady state conditions valid during each discrete time-step of the calculation.

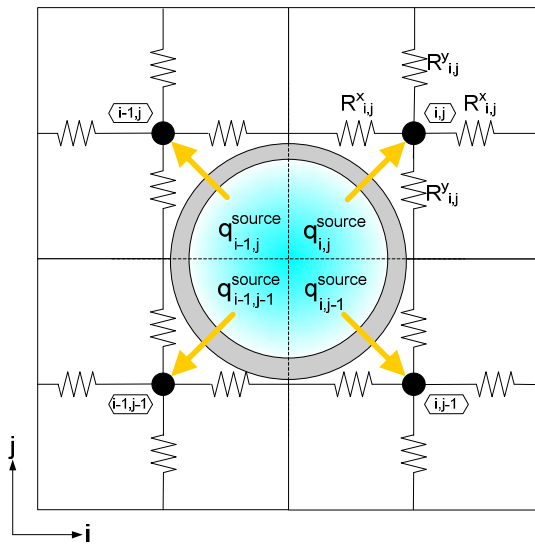


Figure 8 Projection of an embedded pipe segment in between four quadratic pipe inclusion control volumes. These four control volumes are a subset of the whole transversal section plane.

The model for the embedded surface heating element is thermally coupled to a room model through heat convection and long wave radiation exchange at the interior surface of the element. The Net Radiation Exchange model given by Hottel et al. (1967) has been implemented in the existing zone model. The long wave radiation exchange is distributed between internal surfaces according to the surface temperature distribution, surface emissivity and view factors. The algorithm for the Net Radiation Exchange method is given in the licentiate thesis by Karlsson (2006).

The capability to calculate the surface temperature distribution within an enclosure heated by floor heating is illustrated by Figure 9 and Figure 10. The refinement of the spatial grid is also implemented at walls, windows and the ceiling of the enclosure. Hence, the exchange of long wave radiation is calculated for the whole set of subsurfaces. The momentary surface temperature distribution is illustrated by Figure 10. The ability to calculate a refined surface temperature distribution yields the possibility to improve the assessment of thermal comfort within the zone.

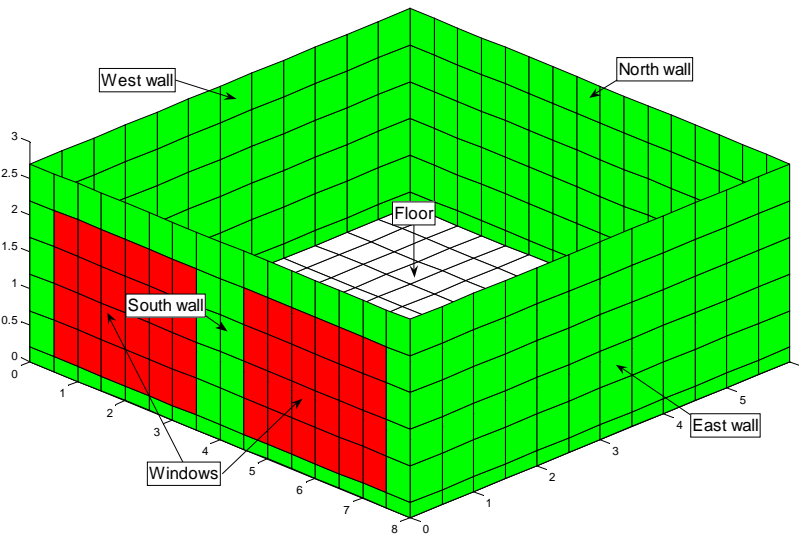


Figure 9 Example of a three-dimensional wire frame model. For details see Paper I.

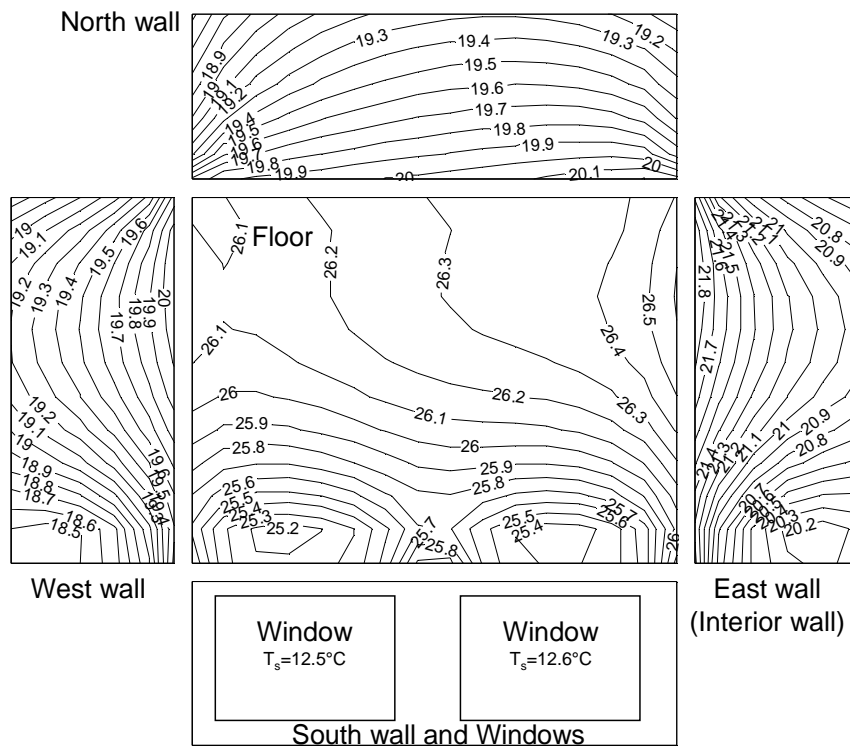


Figure 10 Example of the momentary surface temperature distributions for the floor and walls. The enclosure is fitted with floor heating (uniform heat flux density from the embedded pipe circuit). A Contour line represents a deviation of 0.1°C (contour lines for the south wall and the windows are excluded). For details see Paper I.

The operation of a surface embedded heating system requires a control system which controls the supply fluid temperature and the fluid flow rate through the circuit. An ideal connection to the primary system is assumed. Hence, the exact supply parameters which are determined by the control system are directly implemented to the supply end of the pipe circuit. Due to the modular structure of the Simulink model, an arbitrary number of pipe circuits can be positioned within the same building element. Furthermore, an arbitrary number of embedded surface heating elements can be positioned in the same enclosure. Correspondingly, several pipe circuits are connected to a common supply manifold assembly and a common return manifold assembly. The fluid flow can be individually adjusted for each pipe circuit. The hydraulic condition for the embedded pipe system is not considered; hence, a shift in fluid flow for a single circuit does not affect other circuits in the hydraulic system. The model handles the multi-zone situation where several rooms in a dwelling are simulated simultaneously thanks to the modular structure of Simulink.

2.2 Verification of the Simulink model

The section plane model including the pipe inclusion has been verified by comparing the subsequent heat flux from the pipe circuit with a validated heat transfer software (Blomberg, 1996). A typical floor heating cross section has been studied (12mm wooden floor covering, 100mm concrete slab, 250mm thermal ground insulation, the pipe is positioned 32mm from the insulation and the centre-to-centre distance is 200mm). The results from the steady state comparison are summarised as:

- The total thermal resistance from the pipe towards the interior, in the case of wood flooring, deviated by -0.3 % for a dense section plane discretisation and by +0.8% for a coarse mesh
- The region close to the pipe is studied separately. The numerical error for the simplified pipe inclusion method is only -0.3% in relation to the total thermal resistance for the whole

section plane (dense mesh). A large fraction of the total error in thermal resistance is allocated to the simplified pipe inclusion method.

A response-test was accomplished in order to verify the developed model's transient accuracy. A unit step-change in fluid temperature excites the system. The subsequent transient heat fluxes are compared with a reference solution within one section plane. Hence, the longitudinal heat exchange model is not subject of this verification test. The results for the numerical error in heat exchange between the pipe and the embedding material are summarised as:

- Large relative errors during a short initial period due to limitations in the discretisation of pipe inclusion control volumes (i.e. the node of the pipe inclusion control volumes must be located outside the embedded pipe)
- The relative numerical error never exceeds $\pm 0.7\%$ for a dense discretisation (after an initial time period of 175s)
- The relative error reaches its maximum amplitude at -5.1% after 36min in the case of a coarse mesh

The upward heat flux at the surface is of major importance since it corresponds to the useful heating of the room. The delay time between the step-change in fluid temperature and the increase in surface heat flux precludes a relative comparison during an initial period. The results for the numerical error in surface heat flux and surface energy transfer are summarised as:

- The surface energy transfer is assessed with high accuracy before the surface heat flux has increased to a significant level
- The dense mesh yields a 4% accuracy in surface heat flux after 22min although the surface heat flux has only reached 6.1% of the steady state value after such short time period
- The relative error in surface energy transfer is less than $+2.5\%$ after one hour of operation and $+0.7\%$ after ten hours of operation for the dense mesh; the coarse mesh yields $+2.3\%$ and -1.7% .

Prior to this study, Caccavelli et al. (1994 and 1995) experimentally derived reference data for the specific setup of concrete embedded floor heating. This data is utilised in order to experimentally validate the developed embedded surface heating model in the case of concrete embedded floor heating. The test is performed in a test cell where the indoor temperature is controlled by ventilation in order to yield a fairly constant boundary condition at the top surface of the floor element, see Figure 11. The transient thermal response of the system is tested in both long (16 h) and short (30 min) cycle experiments where the water flow rate alters between on and off.

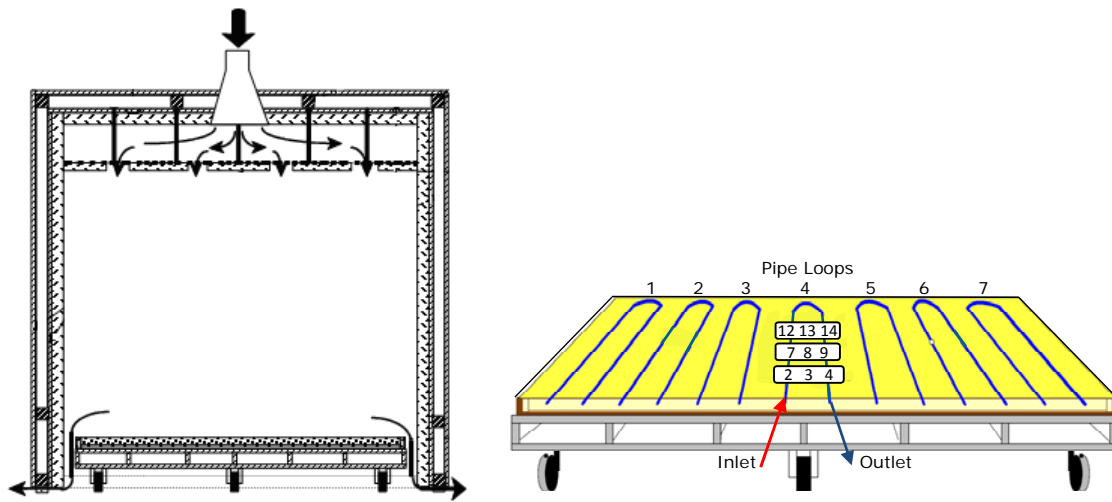


Figure 11 The experimental test cell and the floor construction with indication of measurement locations (Caccavelli et al., 1994).

An overall heat balance computation for the entire test cell is not possible since the air exchange rate of the test cell is not measured explicitly; the model validation is therefore limited to the embedded surface heating element. Surface temperatures at the walls and the ceiling, air temperature within the test cell, operative temperature underneath the floor (casted on top of removable test bench, see Figure 11) and the supply water temperature to each pipe circuit are measured during the experiments. The set of measured values corresponds to the complete set of boundary conditions. The supply temperature is fairly constant at $+36^{\circ}\text{C}$ and the temperature decline is in the range of 3.3°C . Hence, the system operates in the range of the maximum heat supply which is seen at the surface temperatures (i.e. in the range of $+28$ to $+25^{\circ}\text{C}$). Another set of measurement points are utilised in order to validate the model; the temperature of the return water (during pump operation) and the entire set of measurement points along the pipe loop at different heights (TS, TH, TB and TI according to Figure 12).

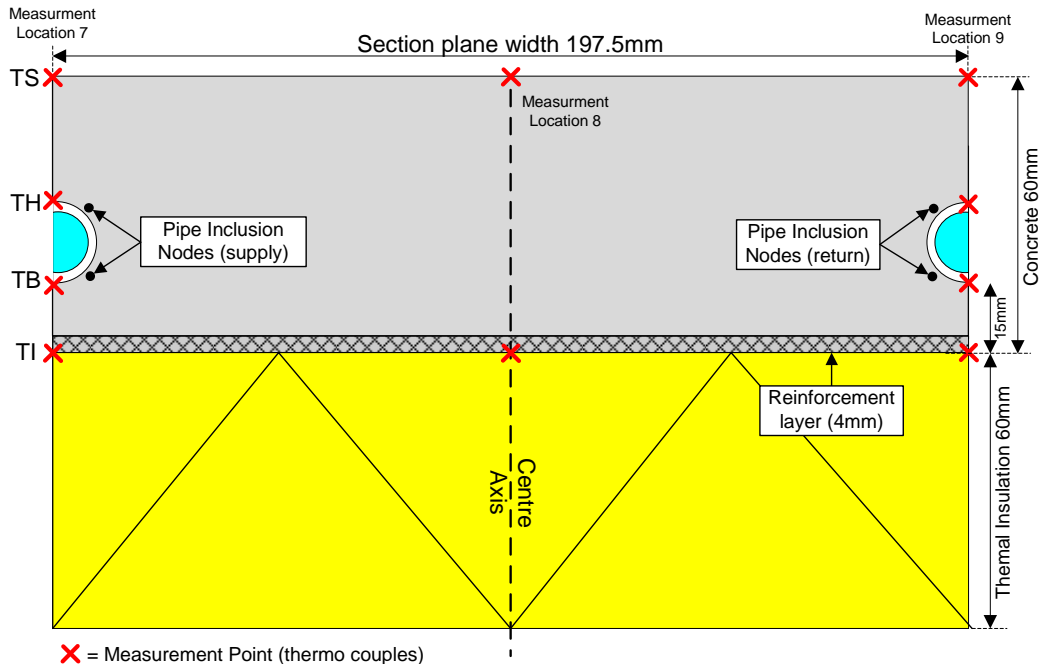


Figure 12 Location of measurement points in the transversal section plane.

Selected results for the reference simulation are presented here. Measured and calculated temperatures at measurement location 7, 8, 9 and at the outlet of the pipe loop are given for the long cycle experiment, see Figure 13. The simulated transient response yields matching results when the shapes of the response curves are considered. The response is initially (i.e. first two hours) slightly faster at measurement point 7, which is closer to the supply, than at location 9. The response between the pipes (i.e. location 8) yields a delay time and prolonged response which is assessed by the model. The model assesses the temperature amplitudes in the short cycle experiment with good precision, see Figure 14. Furthermore, the difference in amplitude among the measurement points is also correct; hence, measurement points close to the embedded pipe fluctuates with higher amplitude than measurement points further way.

Common for long and short cycle tests (reference simulation) is that the model underestimates the heat exchange between fluid and the element (i.e. by 16% at the end of the long cycle test, see the outlet temperature in Figure 13). Surface temperatures are generally assessed with good precision. However, the temperatures in the core of the slab are generally underestimated in both tests (i.e. 0.3 to 1.5°C in the long cycle experiment).

Several causes for the observed deviation in temperature levels between the surface and the core as well as the deviation in heat exchange are discussed in Paper V; a résumé is given here. Unfortunately, the thermal resistance between the pipe loop and the interior is not large due to the lack of floor covering; hence, the relative importance of the choice of convective surface heat transfer model is large. The choice of convective surface heat transfer model is believed to be an important reason for the deviations observed due to the uncertainties induced by possible forced convection. The estimated air exchange rate due to the design of the experiment is much higher than in a residential building. Furthermore, there is a list of other possible causes: influence from pipe sagging between mounts, location of thermocouples (i.e. TH and TB) in relation to the possible location determined by the calculation nodes in the model (see locations in Figure 12), influence on the temperature field due to the steel reinforcement mat, thermal film resistance due to the present flow regime in the pipe. Several of these scenarios are tested one by one in a sensibility analysis. The resulting shift in temperatures and heat exchange for each of the tests corresponds to what one would expect. However, none of the causes can individually explain the observed deviations.

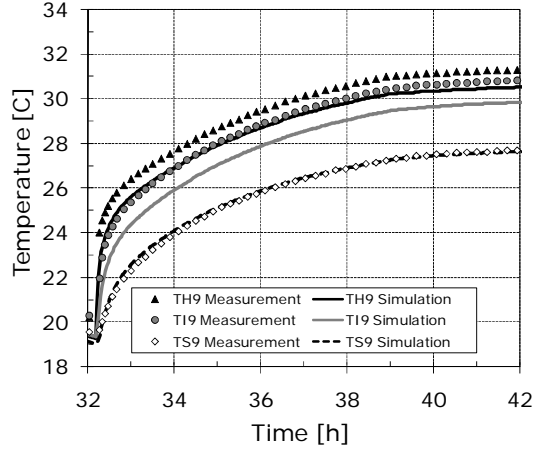
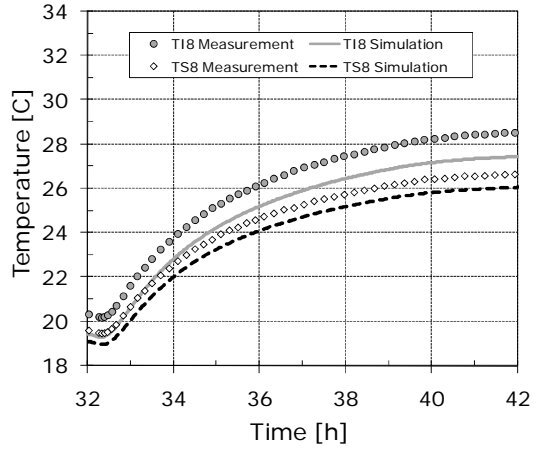
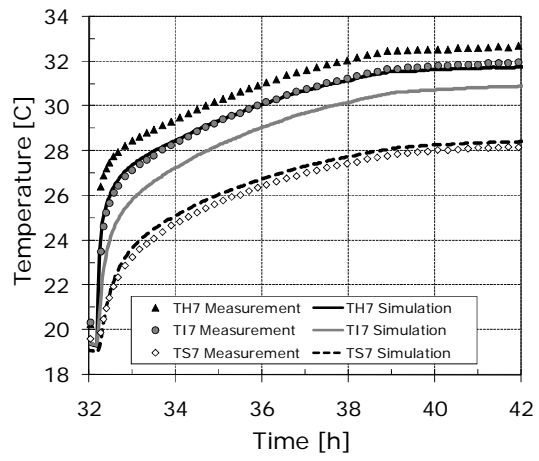
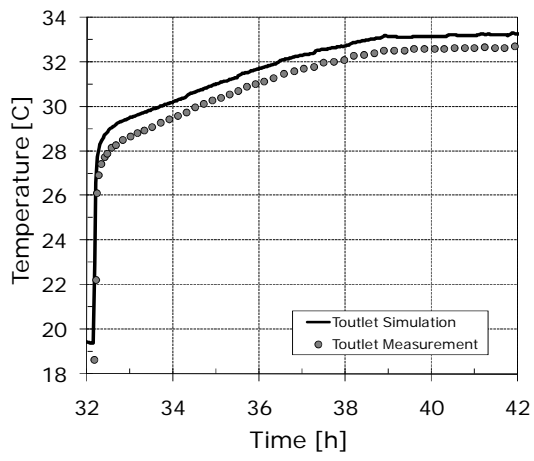


Figure 13 Measurement and simulation of the transient long cycle test. Results for measurement point 7, 8 and 9 are presented.

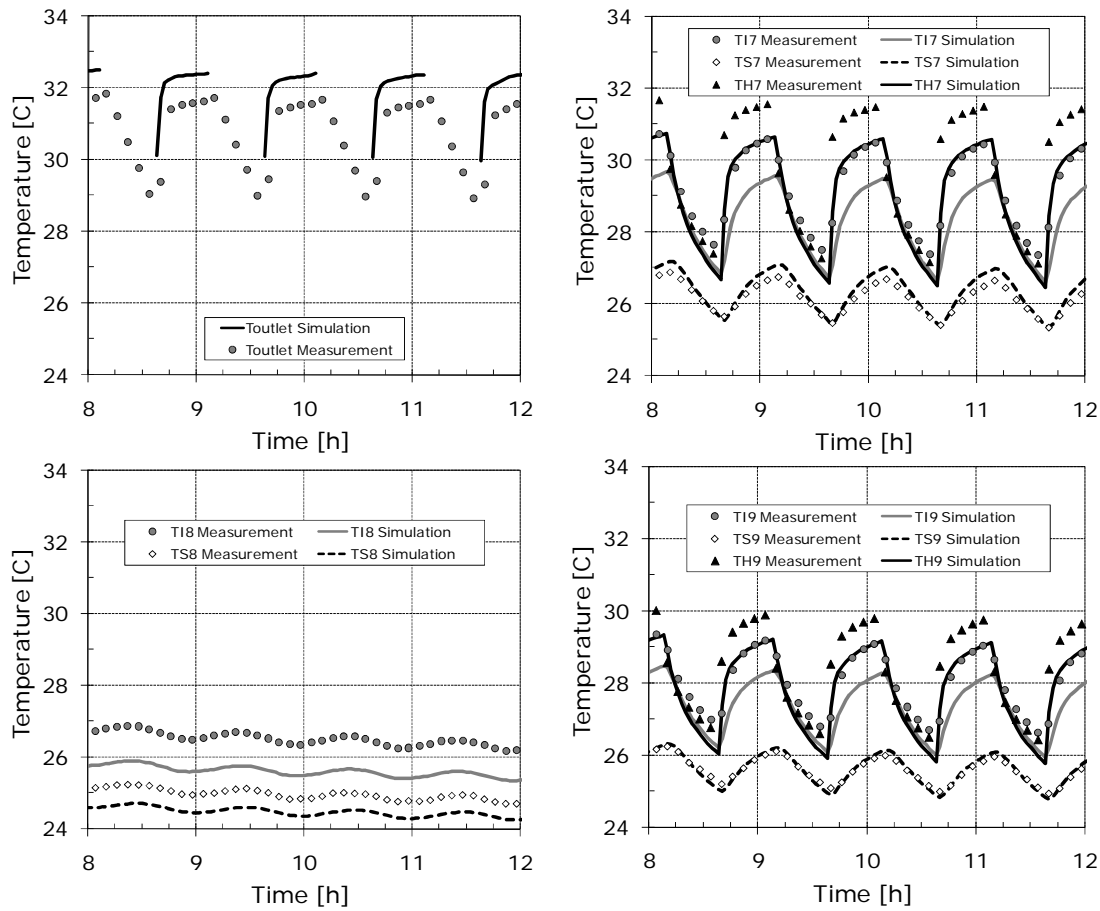


Figure 14 Measurement and simulation of the transient short cycle test. Results for measurement point 7, 8 and 9 are presented.

2.3 Simplified lumped 2-node model

A simplified lumped 2-node model is studied, see Figure 15. The heat capacity and the temperature of the entire floor heating element are lumped in one single lower node (fh). The temperature and heat capacity of the indoor air volume and the material on the inside of the thermal insulation (excluding the floor structure and material facing the exterior) is lumped in one single upper node (i). The parameter in the lumped model has a direct physical meaning: C is the lumped heat capacity of each node, K_{fh} is the thermal conductance between the depth of the pipe circuit and the interior (i.e. including the combined surface heat transfer coefficient for convection and long wave radiation), K_e is the total thermal conductance for conductive and ventilation heat losses and η is the insulation efficiency of the floor element.

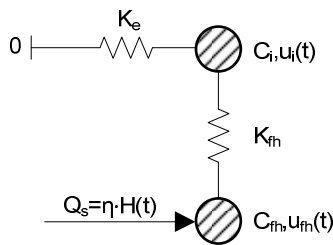


Figure 15 Thermal network illustrating the step-response of the lumped 2-node model.

The model is applied in order to describe the transient relation between the supply heat flux and the subsequent response in indoor temperature. The solution for the non-dimensional step-response indoor temperature $u_i(t)$ is given by an explicit formula, see Equation 1. Two exponential terms determines the transient properties of the system. $t_{c, fh}$ expresses the time shift between the lumped temperature of the floor heating slab $u_{fh}(t)$ and the lumped indoor temperature $u_i(t)$. The parameter b expresses the magnitude of the initial reduction of the non-dimensional step-response temperature during the initial step-response process which is approximately $0 \leq t < t_{c, fh}$. The characteristic time $t_{c, i}$ refers to the time span required to attain steady state conditions where the heat losses are balanced by the heat supply system. As an example, calculations of the parameters for the reference room is given in Paper VII; the characteristic time $t_{c, i}$ becomes 3.23 days, $t_{c, fh}$ equals 3.0h and the parameter b attains a value of -0.041. The lumped 2-node model yields a step-response function $u_i(t)$ that agrees very well with the solution obtained from the Simulink model, see Figure 16. The simplified model is surprisingly accurate in the case of the reference room. Especially the initial delay time (i.e. $t_{c, fh}$) as the heat front conducts from the depth of the pipe circuit towards the interior is included in the two-node model.

$$u_i(t) = \frac{\eta}{K_e} \cdot \left(1 - \left((1+b) \cdot e^{-\frac{t}{t_{c,i}}} - b \cdot e^{-\frac{t}{t_{c, fh}}} \right) \right) \quad (1)$$

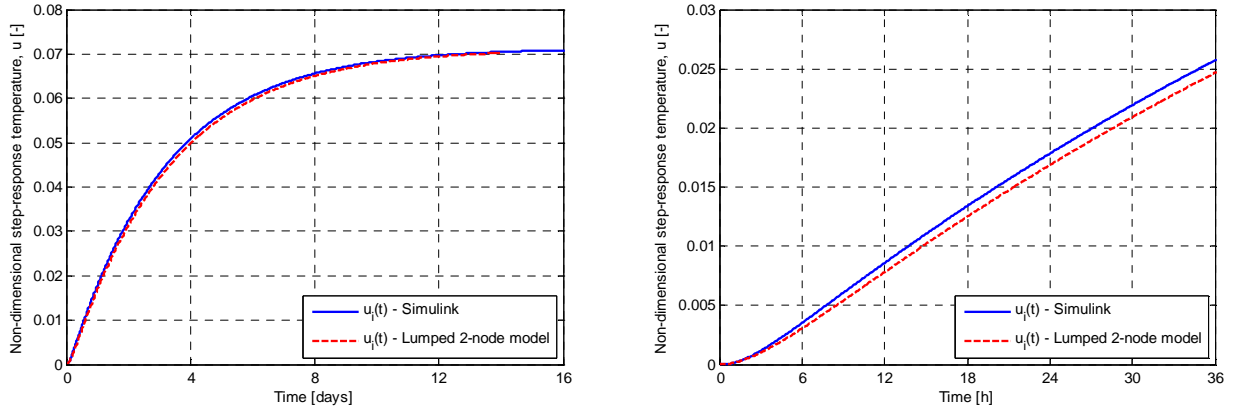


Figure 16 Non-dimensional step-response temperatures $u_i(t)$ (operative indoor temperature) calculated by the lumped 2-node model and the reference Simulink model. The left-hand side illustrates the long term response during 16 days and the right-hand side illustrates the initial 36h.

3 Determination of the supply fluid temperature

The methods and results given in this section summarises Paper VII.

3.1 Optimised supply fluid temperature

Paper VII describes a model based predictive control method which calculates the optimal supply fluid temperature $T_s(t)$ based on the transient properties of the floor heating element and a prediction of the approaching heat demand. The objective is to keep the upcoming indoor operative temperature $T_i(t)$ within a pre-defined comfort interval and at the same time constrain the supply heat flux $Q_s(t)$ within practical limits. For instance, $Q_s(t)$ should not obtain a negative value or impractical high heat flux amplitudes.

The basic structure of this so-called Model Based Predictive control method is given by Figure 17; four main elements are identified in the method. The optimising element is the core of the method. The optimal and constrained $Q_{s,op}(t)$ is iteratively calculated according to the desired objectives (comfort interval and heat supply constraints) and the inherited limitations from the transient properties of the floor heating element. The optimisation element rely on a model which describes the transient relation between $Q_s(t)$ and the subsequent response in the indoor temperature $T_{i,+}(t)$. The prediction element describes the upcoming heat demand through the free-running indoor operative temperature $T_{i,free}(t)$. Finally, the optimal supply heat flux $Q_{s,op}(t)$ is transformed into the corresponding optimal supply fluid temperature $T_{s,op}(t)$.

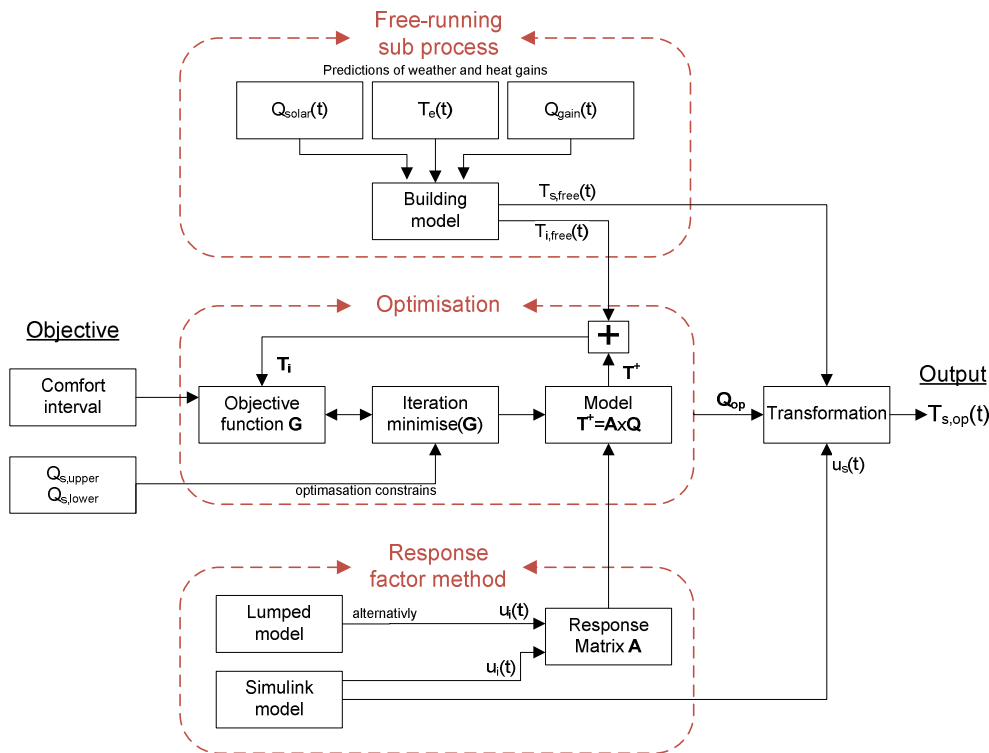


Figure 17 Block diagram illustrating the model based predictive control scheme.

The applied method considers the available prediction of heat gains and the outdoor temperature as a perfect prediction for all times. The prediction is expressed by the free-running indoor temperature $T_{i,free}(t)$ which arises under the influence of the heat gains, solar radiation and the outdoor temperature if the heat supply to the floor heating system is turned off for all times. $T_{i,free}(t)$ represents the base level from which the heating system should shift the indoor temperature to an acceptable level. An assumed perfect prediction, results in a free-running process that is quantified in advance for all times.

The model which describes the transient relation between $Q_s(t)$ and the indoor temperature increase from the base level $T_{i,+}(t)$ is crucial in the applied method. The model must be rapid in order to find the optimal $Q_{s,opt}(t)$ by iteration. On the other hand, it must accurately describe the dynamics of the system. A discrete response factor method fulfils these requirements and is therefore implemented. Hence, the heat supply to the pipe circuit is assumed step-wise constant (i.e. a continuous sequence of heat pulses with width t_p and amplitude q^n). The momentary temperature increase at time $t = m \cdot t_p$ due to the past sequence of heat pulses is given by $T_{i,+}^m$. Thus, the transient indoor temperature is evaluated as a string of discrete values T_i^m , see Equation 2.

$$T_i^m = T_{i,free}^m + T_{i,+}^m \quad (2)$$

The response factor method utilises the elementary non-dimensional step-response function $u_i(t)$, see Figure 16. The $u_i(t)$ function is the resultant indoor operative temperature due to a unit step-change excitation in supply heat flux. The shape of the step-response function is given by the transient properties of the combination of floor heating element and building. The step-response function is calculated by a reference model. Restrictions in the reference model are inherited into the shape of the response function. In this study is either the Simulink model or the simplified lumped 2-node model applied as reference models in order to calculate $u_i(t)$. The continuous $T_{i,+}(t)$ due to an arbitrary continuous $Q_s(t)$ is given by using a convolution formula, see Equation 3. In comparison to the numerical Simulink model, the response factor method significantly reduces the computational requirement which is a must in order to find an optimal supply heat flux through iteration.

$$T_{i,+}(t) = \int_0^t Q_s(\tau) \cdot \frac{du_i}{dt}(t-\tau) d\tau \quad (3)$$

Discrete values of the elementary step-response function are applied in order to compose a discrete pulse-response function; $u_{i,p}^n(t_m)$ is the momentary indoor temperature at time $t_m = t_p \cdot m$ due to the single unit heat pulse which ends at time t_n , see Equation 4. $u_{i,p}^n(t_m)$ is exemplified for at t_p equal to 24h by Figure 18.

$$u_{i,p}^n(t_m) = \begin{cases} u_{i,p}^n(t_p \cdot m) = u_i(t_p \cdot (m-n+1)) - u_i(t_p \cdot (m-n)) & t_p > 0, \quad m \geq n \\ 0 & \text{otherwise} \end{cases} \quad (4)$$

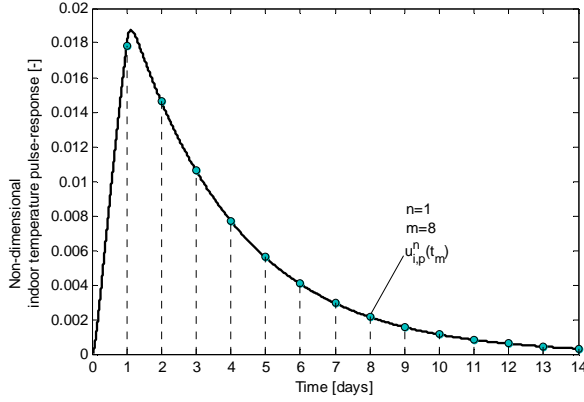


Figure 18 Example of a calculated (Simulink) pulse-response $u_{i,p}(t)$ for a period time of 24h. The pulse excites the system between 0h-24h (i.e. the pulse is denoted $n=1$). Momentary values at time $t_m=t_p \cdot m$ is illustrated by the sequence of circular markers. We exemplify the momentary value $u_{i,p}$ at $t_m=8t_p$ ($m=8$).

The momentary increase of the indoor temperature $T_{i,+}^m$ at time t_m is given by the sum of the previous sequence of single heat pulse responses according to the principle of superposition, see Equation 5. $T_{i,+}^m$ is given by a discrete weighting of the heat supply amplitudes where the elementary single pulse response is utilised as time weighting function. The amplitude of the n^{th} heat pulse is given by q^n .

$$T_{i,+}^m = \sum_{n=1}^{n=m} q^n \cdot u_{i,p}^n(t_m) \quad (5)$$

The string of $T_{i,+}^m$ for all times between $0 \leq t \leq t_p \cdot M$ can be obtained through the matrix operation (Equation 6) where $M \cdot t_p$ represents the final time of interest. The elements of matrix \mathbf{A} , $a^{m,n}$ are given by the elementary single pulse-response according to Equation 4. For a given system and a given piece-wise constant heat supply, the sequence of discrete $T_{i,+}^m$ is rapidly calculated through a matrix multiplication.

$$\mathbf{T}^+ = \mathbf{A} \times \mathbf{Q} \quad (6)$$

$$\mathbf{T}^+ = \begin{bmatrix} T_{i,+}^1 \\ \vdots \\ T_{i,+}^m \\ \vdots \\ T_{i,+}^M \end{bmatrix}, \quad \mathbf{Q} = \begin{bmatrix} q^1 \\ \vdots \\ q^n \\ \vdots \\ q^M \end{bmatrix}, \quad \mathbf{A} = \begin{bmatrix} a^{1,1} & 0 & \dots & \dots & 0 \\ \vdots & \ddots & 0 & \vdots & \vdots \\ a^{m,1} & \vdots & \ddots & 0 & \vdots \\ \vdots & \vdots & \vdots & \ddots & 0 \\ a^{M,1} & \dots & a^{M,n} & \dots & a^{M,M} \end{bmatrix}$$

Generally for the response factor method, the governing equations must be linear since the principle of superposition is utilised. Hence, a constant convective surface heat transfer coefficient h_{conv} is

assumed. The radiative heat exchange is approximately linear as long as the indoor temperature is close to the reference level which is applied during the calculation of the elementary response function $u_i(t)$. Furthermore, the volume flow rate in the embedded pipe circuit cannot change in relation to the constant volume flow rate applied when the elementary step-response function $u_i(t)$ is calculated.

The objective of the method is realised by the comfort interval $[T_{i,lower}(t), T_{i,upper}(t)]$. The method aims to keep the temperature within this interval. The wider the comfort interval is the easier is the control task. The interval approach is more feasible than a fixed set point temperature which is a very strict target. Based on the comfort interval, we define an objective function G which expresses the norm of the momentary temperature deviation which emerges during the considered time span $0 \leq t \leq t_M$, see Equation 7. Constants β_{upper} and β_{lower} express the penalty due to the momentary deviation between the net indoor temperature T_i^m and the upper or lower bounds respectively. The operation interval $[Q_{s,lower}, Q_{s,upper}]$ constrains the heat supply. The lowest possible heat supply amplitude $Q_{s,lower}$ is usually equal to zero, and the upper bound $Q_{s,upper}$ is usually given by the design heat power.

$$G = \sqrt{\sum_{i=1}^M g(m)^2} \quad g(m) = \begin{cases} \beta_{upper} \cdot |T_i^m - T_{i,upper}^m| & T_i^m > T_{i,upper}^m \\ \beta_{lower} \cdot |T_i^m - T_{i,lower}^m| & T_i^m < T_{i,lower}^m \\ 0 & T_{i,lower}^m \leq T_i^m \leq T_{i,upper}^m \end{cases} \quad (7)$$

The series of momentary T_i^m is calculated iteratively by utilising the rapid response factor method until the solution converges into one optimised solution $Q_{s,op}(t)$ which minimises the objective function during the upcoming time sequence. $T_{i,op}(t)$ is the optimised indoor temperature which is within the comfort interval for as long time as possible. The optimisation problem is solved by applying the *fmincon* Matlab function which numerically finds the minimum to a constrained non-linear multivariable function. The optimisation method makes use of the prognosticated $T_{i,free}^m$ during the whole considered time sequence.

The final step in the method is to transform the supply heat flux into the corresponding supply fluid temperature; Paper VII yields a general transformation method for a continuous $Q_s(t)$. The elementary non-dimensional supply fluid temperature $u_s(t)$ due to the unit step-change in supply heat flux is needed in the transformation. $u_s(t)$ needs to take into account the transient properties of the pipe circuit and is therefore calculated by the detailed Simulink model. The transformation is an essential part of the studied control method since the aim is to determine the optimal supply fluid temperature $T_{s,op}(t)$ rather than $Q_{s,op}(t)$. The reason is that the self-regulation ability of the floor

heating element is only possible if $T_s(t)$ is the controlled supply variable. However, $Q_{s,op}(t)$ is utilised as a transition variable within the optimisation algorithm since it greatly simplifies the implementation of heat supply constrains.

A transient case study is given in Paper VII where the method is tested; selected results for a 10 day period are given in order to exemplify the outcome of the optimisation algorithm. The considered free-running sub process is given by Figure 19. The comfort interval is defined as $+20^\circ$ to $+22^\circ$ and the supply heat flux is constrained within 0 to 35 W/m^2 . The applied method is based on a period time of 2h. Two optimised solutions $Q_{s,op}(t)$ are illustrated; one with elementary response function obtained from the Simulink model and one that is obtained from the lumped 2-node model. The results are very similar; hence, the lumped 2-node model is applicable as a simplified tool in order to calculate the elementary step-response function $u_i(t)$. $T_{i,free}(t)$ is quite stable in comparison to the applied comfort interval. However, there is a peak in solar gains which is followed by a cold spell during the 44th-45th day of the year which clearly shows the operation of the optimised control. This event causes the free-running indoor temperature to increase followed by a rapid decrease of approximately 5°C , see Figure 19. As seen, the heat supply first decreases in order to counteract the solar gain followed by an increase in order to counteract the cold spell during the night. At this stage $Q_s(t)$ is limited by $Q_{s,upper}$. Finally, the heat supply is reduced during the later stage of the cold spell in order to avoid over-temperatures afterwards.

The transformation from the $Q_{s,op}(t)$ into the corresponding $T_{s,op}(t)$ is given for the Simulink solution $Q_{s,op}(t)$, see Figure 21. The optimal supply fluid temperature is relatively stable over the considered time period. The shifts in supply temperature during the cold spell are within a few degrees. Finally the continuous $T_{i,op}(t)$ is calculated by the Simulink model. The indoor temperature is within the desired comfort interval during most of the studied time period, see Figure 22. The upper limit of the comfort interval is exceeded during the transient period at day 44 and 45. The temperature difference caused by the different choice of elementary step-response function (i.e. lumped 2-node or Simulink model) can also be seen in Figure 22.

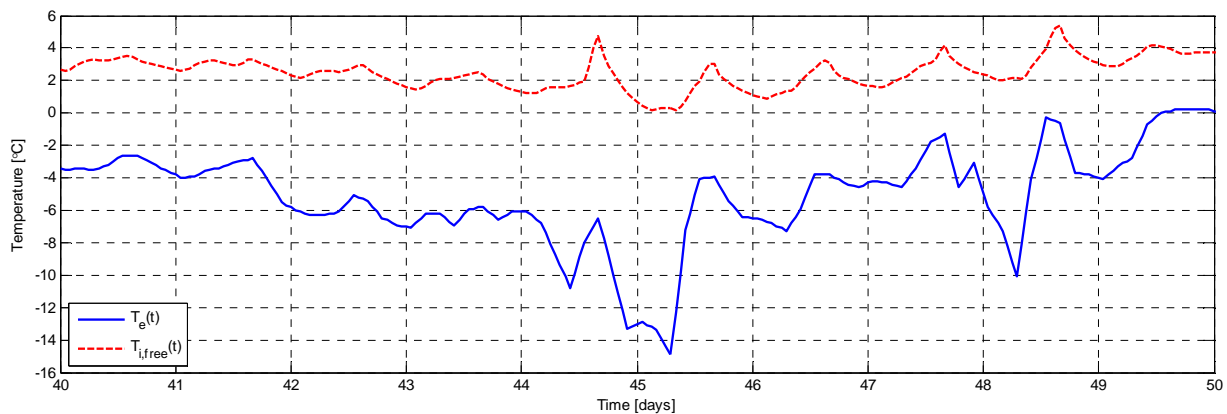


Figure 19 The considered free-running indoor temperature and exterior temperature.

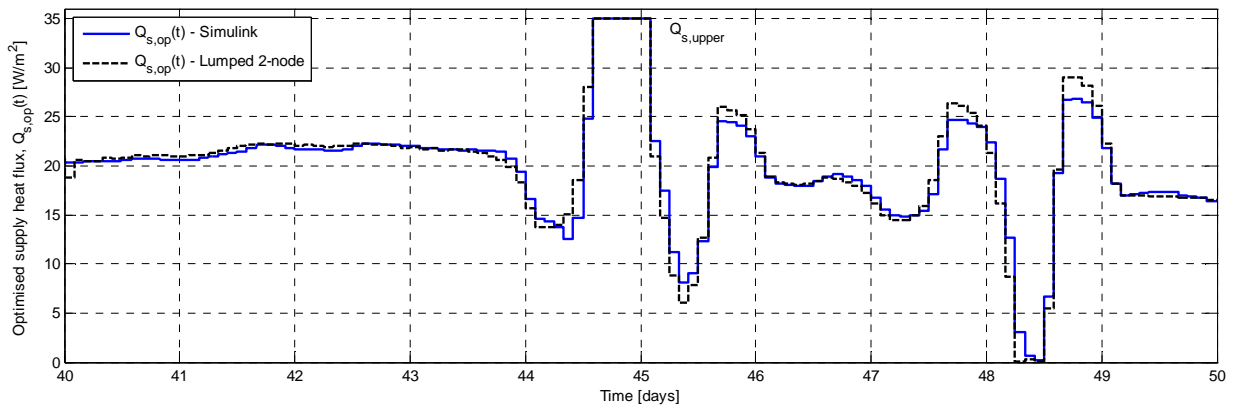


Figure 20 Optimised supply heat fluxes during the considered time period.

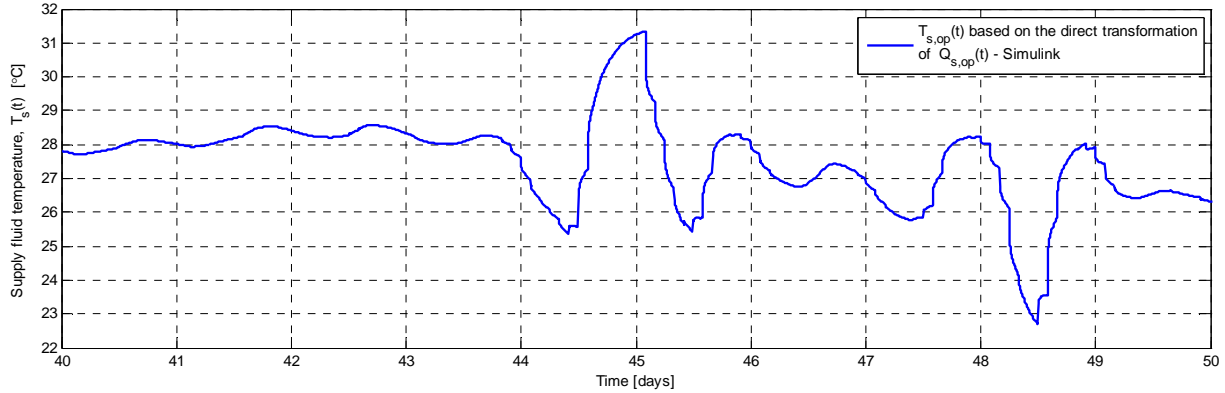


Figure 21 The corresponding optimal supply fluid temperature during the considered time period. The transformation is calculated with a 60s discrete time-step.

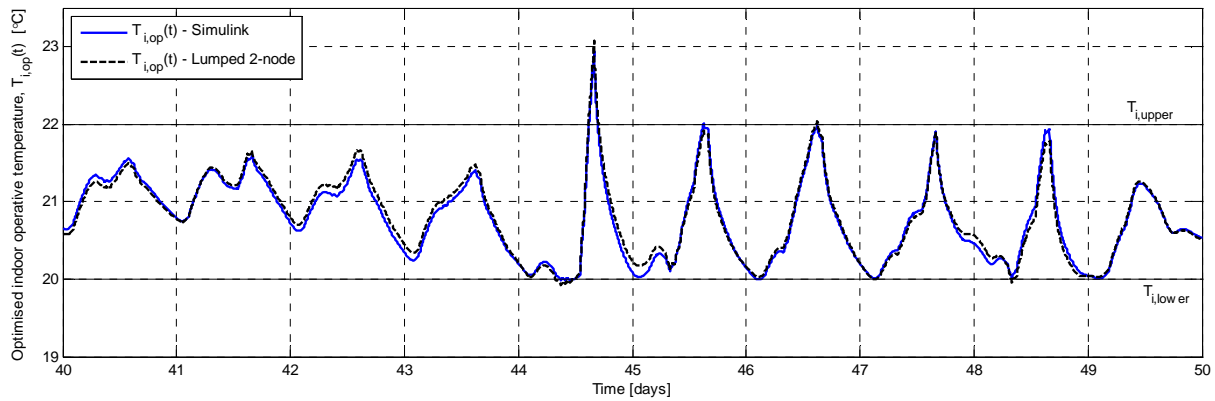


Figure 22 The calculated (i.e. by Simulink) resultant indoor temperature due to the optimised heat supply parameters.

3.2 Simplified methods in order to calculate the heat supply

Alternative solutions in order to calculate $Q_s(t)$ have been explored in Paper VII. The linear equation system defined by Equation 6 can be straightforwardly solved. However, the equation system becomes nearly singular for short t_p which cause very large and fluctuating heat supply amplitudes. A study of the condition number of matrix \mathbf{A} yields that t_p must be larger than the characteristic time scale $t_{c, fh}$, which is determined by the simplified lumped 2-node model. The studied reference room yields a $t_{c, fh}$ equal to 3h. This corresponds with the results from Hagetoft et

al. (2008); there is no limited and continuous solution $Q_s(t)$ that yields a fixed $T_i(t)$ for all times. The reason is the initial delay caused by the time needed for the heat front to conduct from the depth of the pipe circuit towards the interior.

Calculations for the reference room exemplify the instability problem for shorter t_p . A fixed set point temperature is at 21° and period times of 4h, 8h and 24h are applied for the same 10 days period, see Figure 23 and Figure 24. The resulting momentary indoor temperature fulfils exactly the desired set point at each t_p . However, the obtained supply heat fluxes indicate the problem with this method; t_p must be even longer than $t_{c, fh}$ in order to avoid a fluctuating, or even worse, a negative $Q_s(t)$. Hence, the direct solution of the equation system (Equation 6) has not the ability to follow the dynamics of the heat demand without generating an impracticable $Q_s(t)$.

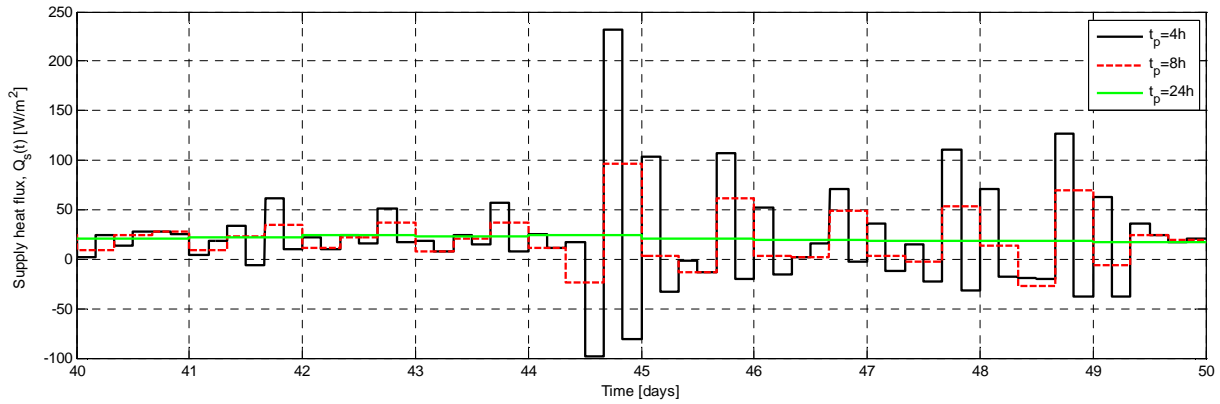


Figure 23 Calculated heat supply series for a 10 days period with period times of 4h, 8h and 24h respectively.

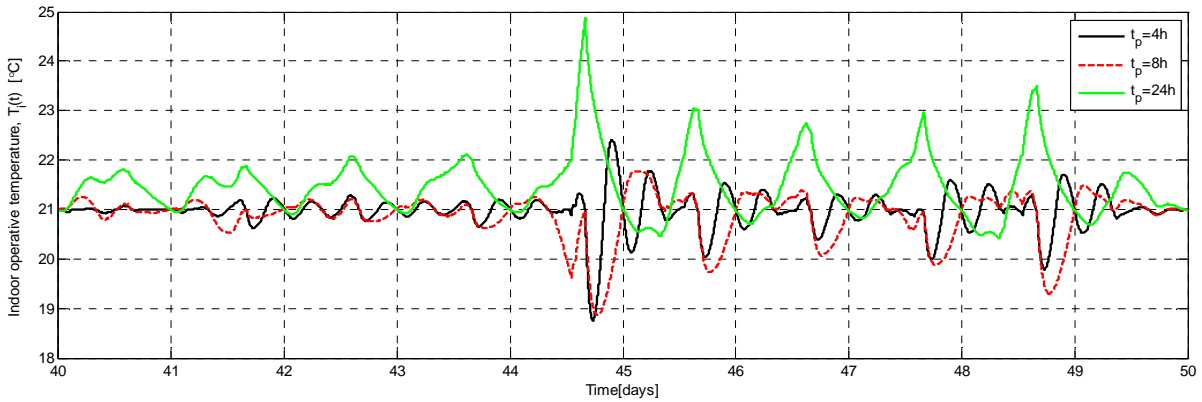


Figure 24 The calculated indoor temperature during a 10 days period for the three heat supply series illustrated in Figure 23.

An explicit formula for the continuous supply heat flux is derived from the lumped 2-node model, see Equation 8. The explicit formula shows that $Q_s(t)$ reaches high values when rapid shifts in the free-running indoor temperature occur. Moreover, the longer characteristic time scales the room and system have the larger heat supply amplitudes are needed.

$$\frac{\eta \cdot Q_s(t)}{K_e} = T_{i,+}(t) - (t_{c,i} + t_{c, fh}) \frac{dT_{i, free}}{dt} - t_{c,i} \cdot t_{c, fh} \frac{d^2 T_{i, free}}{dt^2} \quad (8)$$

The explicit formula is applied in order to calculate the continuous $Q_s(t)$ for the reference room. The desired indoor temperature is constantly 21°C in this example. Figure 25 yields the calculated heat supply during 10 days of system operation. Discrete values each 60s of the free-running indoor temperature and the corresponding time derivatives are considered in this example. The explicit solution $Q_s(t)$ fluctuates with large values of the heat supply flux. Thus, the explicit solution is not practically applicable. The corresponding $T_i(t)$ is calculated by the detailed Simulink model, see Figure 27. The resultant $T_i(t)$ deviates from the desired value of 21°C due to the simplifications associated with the lumped model.

The moving average based on the continuous solution is also considered in an attempt to level out the observed heavy fluctuations. The moving average is based on a 24h period, 12h back in time and 12h ahead in time; see Figure 26. This approach yields an approximate solution with a significant reduction of the heat supply amplitude. The influence of the derivative term and especially the second derivative term decreases by conducting the moving average procedure. The resulting $T_i(t)$ is seen in Figure 27.

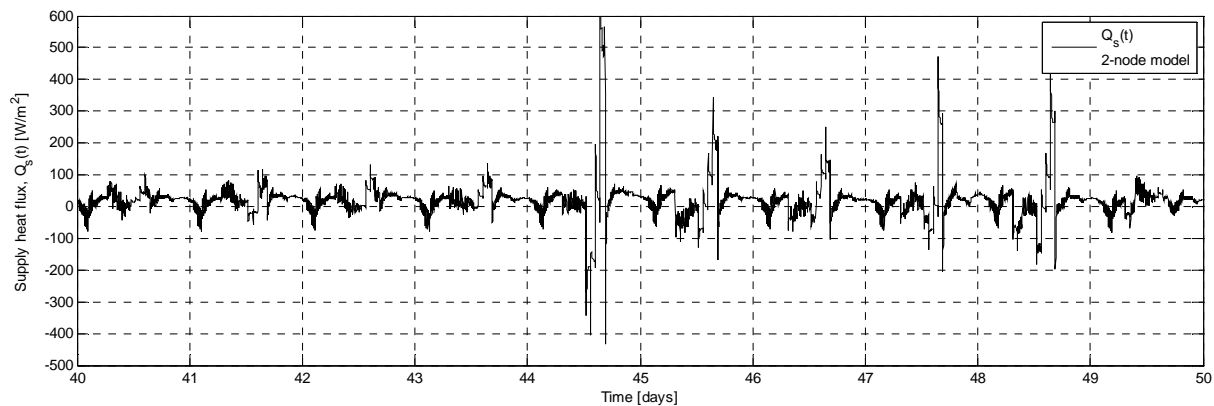


Figure 25 Calculated supply heat flux based on the lumped 2-node model. The result are calculated by Equation 8 (60s discrete time-steps).

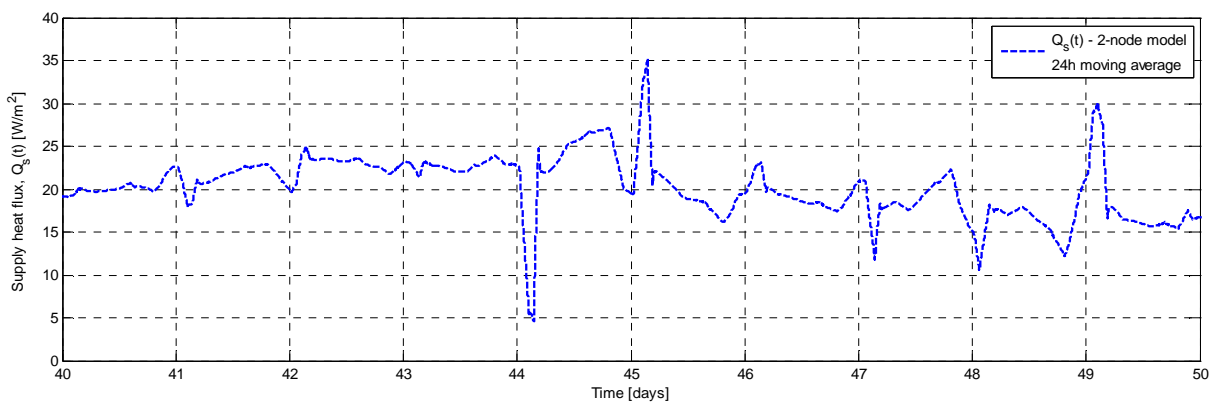


Figure 26 The calculated supply heat flux based on the moving average (24h) of the explicit 2-node solution of $Q_s(t)$.

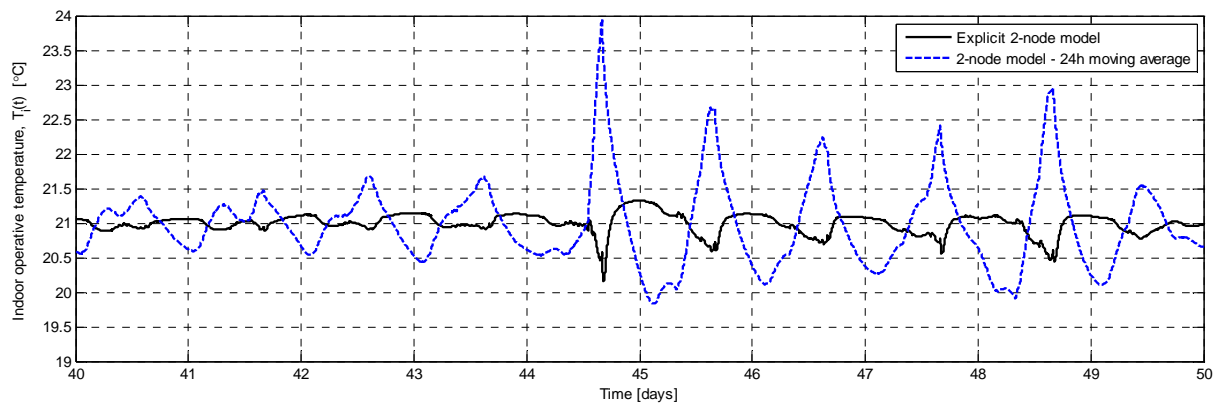


Figure 27 Calculated indoor temperature by the detailed Simulink model based on the heat supply $Q_s(t)$ from the two above given methods (Figure 25 and Figure 26).

The explicit continuous solution derived from the simplified lumped 2-node model and the direct solution to the discrete response function method with a short t_p yields impractical solutions. The slow response from the floor heating element (i.e. the initial delay time) is the cause for the observed behaviour. Practically applicable solutions are only possible if t_p is sufficiently long or the derivative terms are levelled out; hence, the control methods can only follow the daily trend. The model based predictive control method is superior to the other two methods due to the flexible constraint handling capabilities.

4 Self-regulation ability of water-based floor heating

The results from explorative Papers II and III are briefly given in the introduction Section 4.1. Paper VI describes and quantifies the self-regulation ability of floor heating system. Section 4.2 - 4.4 summarises Paper VI.

4.1 Introduction

Paper III explores the self-regulation ability of water-based floor heating system fitted in a residential building without feedback room control. The study considers a very simple control strategy; a constant T_s is supplied to all pipe circuits in the studied multi-zone building. The common T_s corresponds to the average heat demand for the whole building during the coldest month of the year (i.e. February). The calculated supply heat flux responds in the opposite direction whenever the indoor temperature changes due to variations of the heat gain intensity or the exterior temperature, see Figure 28. Hence, the resultant supply heat flux varies indirectly in accordance with the present heat demand. The simulation results are interpreted as an apparent effect of self-regulation. The control of the supply fluid temperature is essential since a corresponding constant supply heat flux wouldn't shift due to the heat demand. The supply heat flux for an individual pipe circuit can be reversed during short periods when high solar gains arise; hence, the pipe circuit extracts heat which is transferred to the common return. This means that a floor heating system with several pipe circuits can transfer heat between individual zones in a multi-zone building. The phenomenon with a locally reversed supply heat flux is explored in a special case in Paper II.

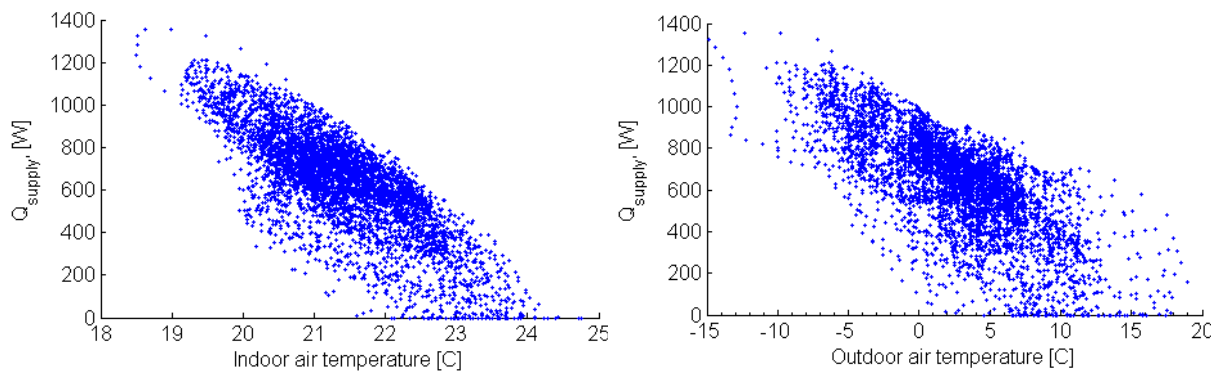


Figure 28 Point diagram illustrating the supplied heat flux to all pipe circuits and air temperatures. On the left-hand side the area weighted indoor air temperature for the entire house is applied. On the right-hand side the outdoor air temperature is applied. Each point represents the average conditions for one hour.

4.2 Transient response analyse

Feed-forward control methods which were studied in Section 3 are based on a bold assumption; a perfect prognosis of the heat gains and the weather exists for all times. The influence of thermal disturbances $\Delta Q_p(t)$ that was not part of the prediction is studied separately. To begin with, the principle of superposition is applied in order to separate the influence of $\Delta Q_p(t)$ from the feed-forwards controlled reference system, see Figure 29. The reference system performs as described in the past Section 3. The supply temperature $T_s^{\text{ref}}(t)$ is feed-forward controlled without feedback control based on the conditions in the room. Hence, the supply temperature for the studied sub process $\Delta T_s(t)$ equals zero for all times and the fluid flow rate is constant and identical for the sub

processes. The exploring of the dynamic system response $\Delta Q_s(t)$ and the net shift in indoor temperature $\Delta T_i(t)$ due to an arbitrary $\Delta Q_p(t)$ constitute an important part of this thesis.

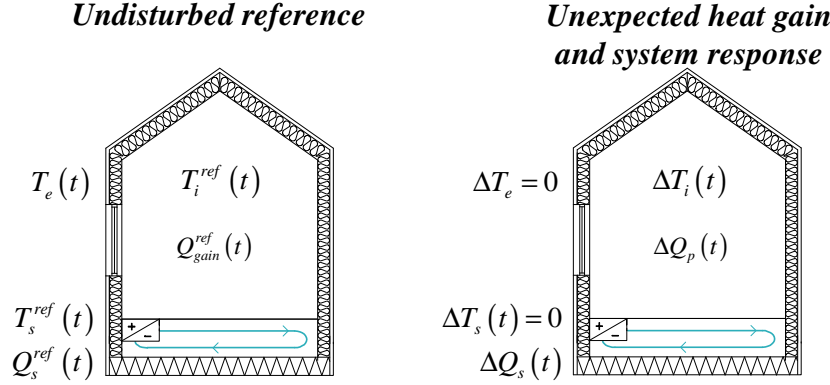


Figure 29 Separation of sub processes by applying the principle of superposition.

The considered sub process (i.e. Δ) is studied with a response factor method in order to quantify the involved transient thermal processes. The convolution formulation given by Equation 9 yields the formula for $\Delta Q_s(t)$ due to an arbitrary $\Delta Q_p(t)$. Past values of $\Delta Q_p(t)$ are weighted to the present value of $\Delta Q_s(t)$ according to weighting functions $f_{III,s}(\tau)$. The weighting function is derived based on the elementary response caused by a unit Dirac impulse in thermal perturbation, see Appendices 1 and 2 in Paper VI. The weighting functions are calculated by the linearised Simulink model with a constant fluid flow rate.

$$\Delta Q_s(t) = f_{III,s} * \Delta Q_p(t) = \int_0^t f_{III,s}(t-\tau) \cdot \Delta Q_p(\tau) d\tau \quad (9)$$

The weighting function describe the integrated transient properties for the combination of room and the floor heating element design. Each unique combination of building and floor heating element yields a unique shape of $f_{III,s}(\tau)$. The reference construction studied in Paper VI yields a weighting function according to Figure 30. Given by the shape of $f_{III,s}(\tau)$, the present intensity of $\Delta Q_s(t)$ does not influence the present heat supply; the same apply for perturbances which were active for more than approximately 50-60h back in time, see Figure 30. The time-distribution of $f_{III,s}(\tau)$ shows that a perturbation which was active for approximately 4h ago has the most influence on the present $\Delta Q_s(t)$. The time weights given by $f_{III,s}(\tau)$ is negative; hence, the shift in $\Delta Q_s(t)$ is always acting contrary to a non-periodic thermal perturbation. The isolated thermal process is a negative feedback process which is called self-regulation. The process is studied in detail in Paper VI. The transient shift in supplied heat flux due to any thermal perturbation is given by two coupled thermal processes. The first thermal process is related to the propagation of heat towards the position of the embedded pipe circuit due to the excitation of a thermal perturbation indoors. The second thermal process is related to the heat exchange along the embedded circuit due to the excitation of the supply fluid temperature. The required supply temperature unite these two processes (i.e. $\Delta T_s(t) = 0$).

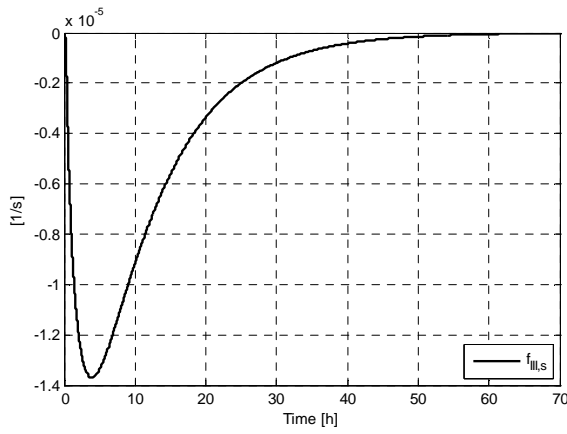


Figure 30 Elementary weighting function $f_{III,s}$.

A self-regulation utilisation factor γ is defined according to Equation 10. The higher absolute value of γ , the more pronounced is the feedback from self-regulation. K_{up} is the equivalent thermal conductance from the supply fluid temperature, over the entire pipe length, towards the interior space. Hence, a significant effect of self-regulation arise if the building envelope and ventilation system yields low heat losses, the thermal resistance of the floor covering is small, the pipe circuit is tightly packed close to the surface of a large interior area and a high fluid flow rate is applied. The net shift in supplied energy $\Delta E_s(\infty)$ due to an arbitrary perturbation with a finite duration time is proportional to the energy content of the perturbation ΔE_p ; γ is the proportional constant, see Equation 11.

$$\gamma = -\frac{K_{up}}{K_e + \eta \cdot K_{up}} \quad , \quad -1 < \gamma < 0 \quad (10)$$

$$\Delta E_s(\infty) = \gamma \cdot \Delta E_p \quad (11)$$

A typical restriction for a residential heating system is that heat extraction is not permitted (i.e. $Q_s(t) \geq 0$). Hence, an upper bound of the self-regulation ability exists for a positive thermal perturbation in the case with a single pipe circuit. The self-regulation response $\Delta Q_s(t)$ cannot increase if the turning point defined by $Q_s(t) = 0$ is reached. However, as given in the introduction 4.1, in a multi-zone application a single pipe circuit can extract heat as long as the net supply heat flux is equal or larger than zero.

A parameter study is performed in Paper VI; the reference room is considered. The fluid flow rate is reduced in case (A), the heat recovery from the exhaust air by-passed in case (B), the wooden floor is exchanged into a stone floor in case (C), the pipe circuit is moved from the bottom to the top of the concrete slab in case (D) and in case (E) is the centre-to-centre distance decreased from 300mm into 150mm (two pipe circuits and the same net fluid flow rate). Each variation affects the weighting function $f_{III,s}(\tau)$, see Figure 31 and Table 1. The results show that self-regulation is an integrated phenomenon which depends on both the design of the floor heating element and the design of the building.

Table 1 Variation of essential input parameters due to the design of each case and the resulting γ .

	K_e	α_{up}/cc	K_{up}	η	γ
	[W/K]	[W/m ² /K]	[W/K]	[-]	[-]
Reference case	13.27	2.83	32.7	0.971	-0.726
Fluid flow (A)	13.27	2.83	23.8	0.971	-0.654
No heat recovery (B)	19.60	2.83	32.7	0.971	-0.637
Stone floor (C)	13.29	3.66	41.4	0.980	-0.768
Pipe mounting height (D)	13.27	3.18	36.4	0.975	-0.746
Half cc (150mm) (E)	13.27	3.55	40.1	0.971	-0.768

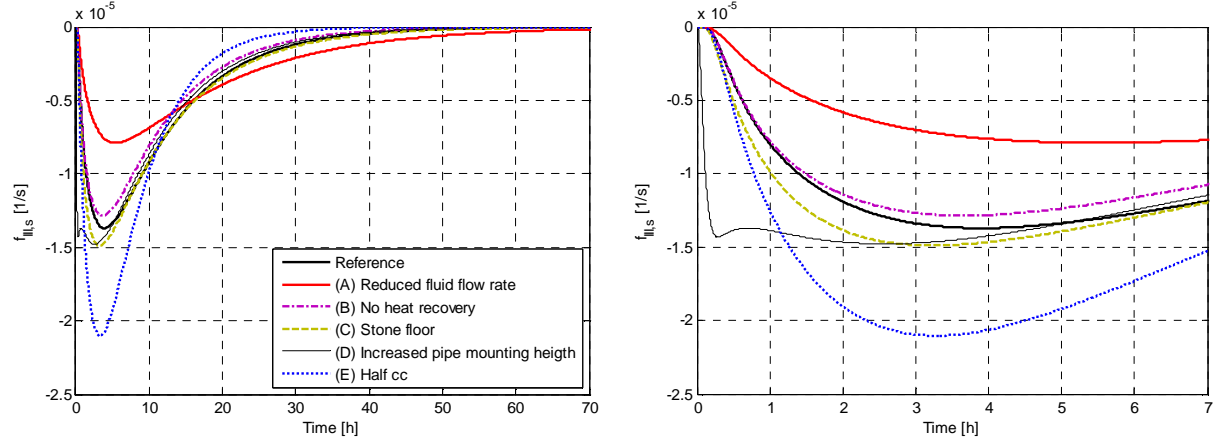


Figure 31 Weighting functions $f_{III,s}$ for all cases in the parameter study. The left-hand side illustrates the whole transient process until 70h after the occurrence of the perturbation. The right-hand side illustrates the initial 7h of the process.

4.3 The consequence on the indoor temperature due to self-regulation

$\tilde{T}_i(t)$ is the indoor temperature caused by the thermal perturbation (i.e. without the counteracting effect from self-regulation). $T_i'(t)$ is the indoor temperature only caused by the counteracting effect from self-regulation. $\Delta T_i(t)$ is the net temperature for the considered sub process (i.e. the sum of $\tilde{T}_i(t)$ and $T_i'(t)$). The steady state net indoor temperature ΔT_i^S due to a constant perturbation is given by Equation 12. The counteracting effect on the steady state temperature due to self-regulation can be significant. As an example, the reference construction yields: $\gamma = -0.726$ and $\eta = 0.971$. Hence, the steady state temperature increase is reduced by 70% as a result of the self-regulation ability.

$$\Delta T_i^S = \frac{\Delta Q_p}{K_e} \cdot (1 + \eta \cdot \gamma) \quad (12)$$

The transient $\Delta T_i(t)$ is given by an analogous convolution formula, see Equation 13. The weighing function $f_{III,i}(\tau)$ comprises the joint effect of the perturbation and the counteracting effect on the indoor temperature due to the self-regulation response. Without giving all details, $T_i'(t)$ is given by

Equation 14; the joint weighting function $f_{l,f} * f_{ll,i}$ describes the counteracting effect from self-regulation, see Figure 33. The effect from self-regulation becomes evident on the indoor temperature after a few hours. The heat front from the perturbation must first reach the embedded pipe. At that time, the system starts to emit a counteracting heat front along the pipe circuit (i.e. the counteracting self-regulation heat flux $\Delta Q_s(t)$ in order to uphold $\Delta T_s(t)=0$). The indoor temperature cannot be affected until the counteracting heat front reaches the surface of the floor heating element.

$$\Delta T_i(t) = f_{ll,i} * \Delta Q_p(t) \quad (13)$$

$$T_i'(t) = -f_{ll,i} * f_{l,f} * \Delta Q_p(t) \quad (14)$$

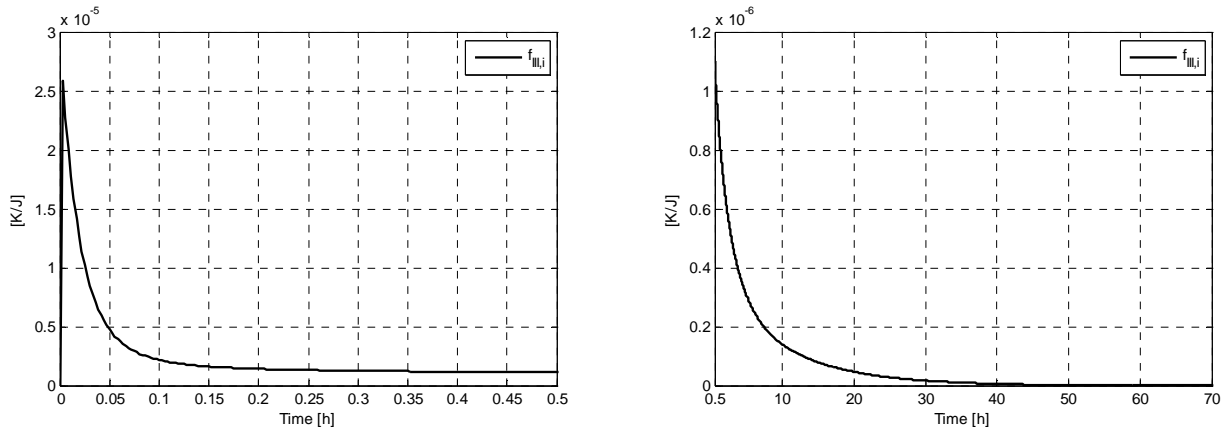


Figure 32 Elementary weighting function $f_{ll,i}$. On the left-hand side: the impulse-response during the first 30min. On the righthand-side: the continued impulse-response from 30min to 70h.

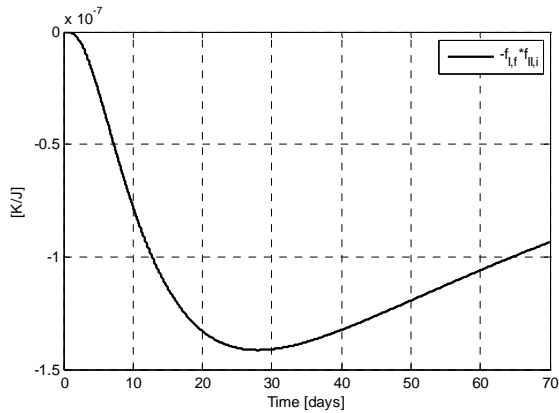


Figure 33 Joint weighing function $-f_{l,f} * f_{ll,i}$, which describes the transient counteraction on the indoor temperature due to the self-regulation response.

4.4 Self-regulation due to periodical perturbances

The indoor temperature amplitude due a periodic perturbation is studied in Paper VI for the reference construction. The net temperature amplitude $\Delta T_i(t)$ is decreased due to self-regulation when the period time is longer than approximately 100h, see Figure 34. However, $\Delta T_i(t)$ is actually increased by the self-regulation effect when the period time is between approximately 12h and 100h. The increase in net temperature amplitude arises due to an unfavourable phase shift which is caused by the delay induced by the transient thermal processes within the floor heating slab. The delay and amplitude of the counteracting effect from self-regulation is given by Equation 14. The self-regulation process is inert for period times shorter than approximately 12h since the periodic heat front from the interior do not reach to the depth of the embedded pipe circuit.

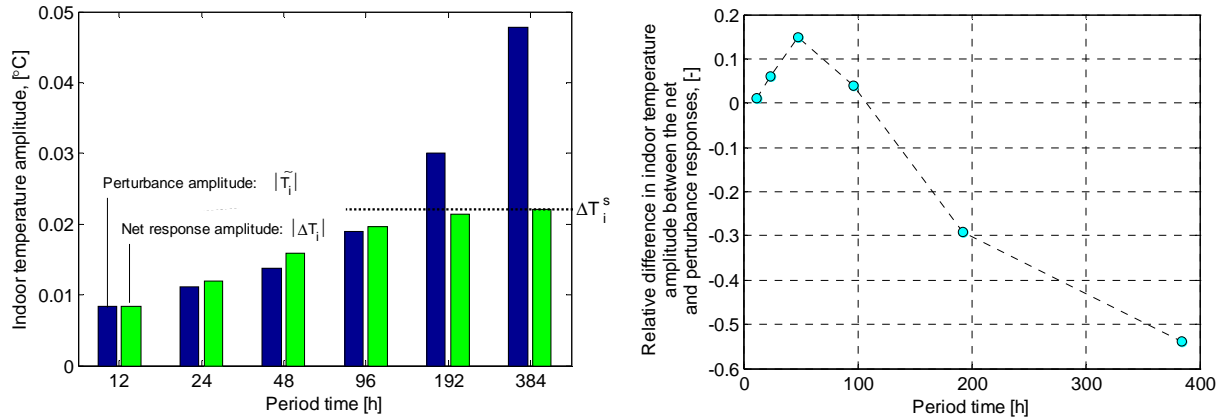


Figure 34 Calculated indoor temperature amplitudes for different period times. The left-hand side illustrates absolute values for the temperature amplitude due to a unit amplitude sinusoidal perturbation and the right-hand side illustrates relative values for the induced shift in temperature amplitude.

5 Conclusion

A numerical simulation tool for water-based embedded surface heating elements is developed and verified. The model is valid for surface heating systems where pipe circuits are embedded within a layer of solid material. The ability to perform a general thermal system analysis where the transient operation of the embedded surface heating system is assessed jointly with all relevant systems (i.e. controls, ventilation, heat gains, building structure etc.) is the main benefit of the developed model. The model's ability to accurately calculate the steady state and transient heat flux from the fluid towards the adjoining embedding concrete and the net heat flux towards the interior where verified by comparing the results with another validated numerical model. Validation tests against published measurements (Caccavelli et al., 1994) have been performed in order to test the model's ability to assess the heat exchange process and temperature field that arise within an embedded floor heating system during transient operation. The validation test is restricted to the model which describes the embedded surface heating element and the special case of embedded floor heating with an uncovered concrete surface. The calculated reference case yields an underestimation of the heat exchange from the pipe loop by -16% in comparison to the measurements at maximum steady state heat output. Generally, for the experimental validation tests temperatures at the core of the concrete slab are underestimated by 0.3 to 1.5°C. At the same time, the set of calculated floor surface temperature matches the set of measured temperatures. The transient test has shown that amplitudes, phase shifts, rise and delay times at different distance from the embedded pipe are assessed with good precision. The influence of material properties, applied boundary conditions and an imprecise construction are tested by means of a sensitivity analysis. None of the tested cases can independently explain the observed general trend in temperature deviations.

A model based predictive control method is applied in order to control the operative temperature in the case of concrete embedded water-based floor heating. The aim is to keep the operative temperature within a comfort interval and at the same time constrain the supply heat flux within practical limits. A discrete transient response factor method is utilised by a numerical optimisation algorithm that iteratively finds the optimal supply heat flux. The response factor method describes the transient relation between a piecewise constant supply heat flux and the succeeding shift in indoor temperature. The basis for the developed method is the elementary response function which can be obtained from an optional model and a prognosis of the upcoming heat demand. A general method which transforms an arbitrary transient supply heat flux into the corresponding supply fluid temperature is derived based on the applied response method.

The optimised predictive control utilises both the knowledge of the transient properties of the heat supply system and the prognosis in an integrated way. Hence, the optimised predictive control has the ability to respond with the best possible action in advance due to an upcoming shift in heat demand and the considered supply constraints. The stability of the system has been studied; the initial delay time caused by the time needed for a heat front to conduct from the depth of the embedded pipe circuit towards the interior sets a limit for the applied period time in the discrete response method. Without the prognosis control and the comfort interval, a limited and stable solution (i.e. sequence of supply heat pulses) exists only if the applied period time is longer than the delay time. However, it has been verified that the applied optimised predictive control converges

into an optimal solution without stability problems although the period time is shorter than the critical delay time.

The explicit and continuous solution to a simplified lumped 2-node model is also considered as a method to find the required supply heat flux. The explicit solution yields a heat supply flux which fluctuates heavily due to the delayed response of the embedded element. Moreover, the simplified 2-node model yields an elementary step-response function which is surprisingly accurate in comparison to the detailed numerical model. Calculations show that the simplified step-response yields an optimised indoor temperature that agrees very well with the results obtained with the detailed step-response.

The response in supply heat flux and indoor temperature due to an unknown thermal perturbation are studied separately from the prognosticated variations by applying the principle of superposition. The system response for a concrete embedded floor heating system with a feed-forward controlled supply water temperature without room control is studied. It has been found that such system responds with a negative feedback process that counteracts any non-periodic thermal perturbation by shifting the supplied heat flux in the opposite direction. The outcome is a more even indoor temperature and enhanced utilisation of heat gains. The feedback process is called self-regulation.

The transient self-regulation process is quantified by means of a response factor method; impulse-responses have been calculated by the detailed numerical model with linearised surface heat transfer coefficients. Fundamental information about the involved thermal processes can be gained from the shape of the impulse-responses. It has been shown that the transient shift in supplied heat flux is given by two coupled thermal processes. The first thermal process is related to the propagation of heat towards the position of the embedded pipe circuit due to the excitation of a thermal perturbation indoors. The second thermal process is related to the heat exchange along the embedded circuit due to the excitation of the supply fluid temperature. These two processes are connected by the demand of an unchanged supply fluid temperature (i.e. from the feed-forward supply temperature control). Hence, self-regulation in the described way is only achievable if the supply fluid temperature is the controlled variable.

For a periodic perturbation, the outcome of self-regulation is dependent on the period time. Short period times yields an inert self-regulation process, intermediate period times yields a small increase in indoor temperature amplitude while longer period times yields a reduced amplitude.

A self-regulation utilisation factor is defined as the ratio between the accumulated shift in supply heat flux and the energy content of a finite thermal perturbation. A building with small heat losses through conduction and ventilation in combination with a high equivalent thermal conductance from the supply of the pipe circuit upwards to the interior yields a high self-regulation utilisation factor. Hence, self-regulation is an integrated phenomenon which depends on both the design of the floor heating element and the design of the building.

6 Further studies

This thesis quantifies the self-regulation feedback and shows that it can facilitate the control of the heating system which stabilises the indoor temperature. It is relevant to study at what level of the self-regulation utilisation factor it is possibility to entirely rely on a simplified feed-forward controlled floor heating system without room control. Such simple system design would lead to cost reductions and a very robust heat supply system.

Other thermal perturbances than convective heat gains are not considered explicitly in the study of self-regulation. Solar gains and radiative heat gains yields a different transient behaviour of the perturbation sub-process. Especially solar gains that incident on the floor surface are believed to yield an initially faster perturbation sub-process. The responses for different perturbances are relevant to study in order to improve the understanding of self-regulation.

Both the study of model based predictive control and the fundamentals for the self-regulation ability are studied in a single room application. However, several pipe circuits with a common supply fluid temperature are usually connected to a common manifold assembly. This will affect both self-regulation and the optimised control of the system. The optimal supply temperature may differ for each pipe circuit. Thus, a study of the integrated design of building and floor heating element which yields a sufficiently even supply fluid temperature distribution between the pipe circuits is relevant. In the case of multi-zone application and self-regulation emerge the possibility do distribute heat between different zones. A deeper analysis of this process would be relevant, especially for well insulated low energy buildings where intensive heat gains easily generate a reversed local heat flux.

Other objective functions than the momentary temperature deviation can be implemented in the optimisation. It is especially interesting to include cost or operation optimisation of the energy supply chains in the supply control of the individual building. Hence, the outcome of such multi-variable optimisation can for instance be that a limited amount of heat can be stored in the floor element during times when the heat production in the primary system benefits from such action and as long as the assessed indoor temperature is acceptable. For instance assisting the district heating system by level out the heat generation through short-time storage or avoiding running a heat pump during the peak electricity load.

The model based predictive control method yields the best possible supply fluid temperature based on the available information. Hence, the optimisation methodology can be utilised in order to evaluate the robustness of simple feed-forward control methods such as a nearly constant supply fluid temperate.

The response factor method relies on the linear assumption which especially influences the convective surface heat transfer. The linear assumption is valid as long as the indoor temperature and interior surfaces are fairly constant. Large temperature fluctuation may induce an error from the linear method which is the basis for both the optimised control and the quantification of self-regulation. A deeper analysis of the validity of the linear assumption is relevant.

7 References

- Bean, R., Olesen, B.W. and Kwang, W.K, (2010). History of Radiant Heating & Cooling Systems – part 1. *ASHRAE Journal*. 40-47.
- Beiron, J., Frodeson, S. and Wikström, F. (2007). *Lågenergihus med 44 lägenheter - Drifterfarenheter, driftstatistik samt miljöbedömning av energianvändning*. Avd för energi-, miljö- och byggt teknik, Karlstads universitet, Karlstad, Sweden.
- Blomberg, T. (1996). *HEAT CONDUCTION IN TWO AND THREE DIMENSIONS Computer Modelling of Building Physics Applications*. Department of Building Technology, Building Physics, Lund University, Lund, Sweden.
- Caccavelli, D., Bedouani, B and Baude, J. (1995). Modelling and dimensioning a hot water floor heating system. *Proceedings of the 4th International Building Performance Simulation (IBPSA) Conference 1995*, Madison, Wisconsin, United States.
- Caccavelli, D. and Richard, P. (1994). *Etude portant sur le dimensionnement d'un plancher chauffant à eau chaude en CIC*. Rapport n°2, n° GEC/DST-94.050R, CSTB, France.
- CEN (2008). *EN 15377: Heating systems in buildings – Design of embedded water based surface heating and cooling systems*. European Committee for Standardization, CEN.
- Chen, T.Y. (2001). Application of adaptive predictive control to a floor heating system with a large thermal lag. *Energy and Buildings* 34, 45-51.
- European Parliament (2009). Press Release, REF. : 20091118IPR64746.
- Eurostat (2009). *Panorama of energy – Energy statistics to support EU policies and solutions*.
- EU-Directive 2002/91/EC of the European Parliament and of the council of 16 December 2002 on the energy performance of buildings. European Commission
- Garcia, C., Prett, D. and Morari, M. (1989). Model Predictive Control: Theory and Practice – a Survey. *Automatica* 25: pp.335–348
- Hagentoft, C.-E., Karlsson, H. and Sasic Kalagasidis, A. (2008). Floor heating in buildings with small energy demand for heating – Feasibilities for the control of the internal temperature using heating. *Proceedings of the Buildings Physics Symposium in honour of Professor Hugo L.S.C. Hens*, 85-89. Leuven, Belgium
- Hottel H. and Sagofirm A. (1967). *Radiative Transfer*. McGraw-Hill, New York, United States.
- Jansson, U. (2008). *Passive houses in Sweden - Experiences from design and construction phase*. Licentiate Thesis, Report EBD-T--08/9. Division of Energy and Building Design, Department of Architecture and Built Environment, Lund University, Faculty of Engineering.
- Joelsson, A. (2008). *Primary Energy Efficiency and CO₂ Mitigation in Residential Buildings*. PhD thesis. Department of Engineering and Sustainable Development, Mid Sweden University. Östersund, Sweden.
- Karlsson, H. (2006). *Thermal system analysis of embedded building integrated heating – numerical model and validation of hydronic floor heating systems*. Thesis for the degree of licentiate of engineering. Chalmers University of Technology, Göteborg, Sweden.

Olesen, B.W. and Langkilde, G. (2009). Calculations of the yearly energy performance of heating systems based on the European building energy directive and related CEN standards. *Cold Climate HVAC 2009 conference*, Sisimiut, Greenland.

Persson, T. (2000). *Lågtemperaturvärmesystem - En kunskapsöversikt*. Solar Energy Research Centre, Högskolan Dalarna, Sweden. (in Swedish)

Roots P. and Hagentoft C.-E. (2005). Released heat from a Line Source in a Foundation Construction. *Proceedings of the 7th Symposium on Buildings Physics in the Nordic Countries*, 839-844. Reykjavík, Iceland.

Sasic Kalagasidis, A. (2004). *HAM-Tools - An Integrated Simulation Tool for Heat, Air and Moisture Transfer Analyses in Building Physics*. Ph.D. dissertation, Building Physics Division, Chalmers University of Technology. Göteborg, Sweden.

Swedish Energy Agency (2009A). *Facts and figures – Energy in Sweden*.

Swedish Energy Agency (2009B). *Summary of energy statistics for dwellings and non-residential premises for 2007*.

Swedish Energy Agency (2009C). *Energy Indicators 2009*.

Swedish Energy Agency et al.. *Grundtips för golvvärme*. ISBN 91-7398-768-9

Weitzmann, P., Sasic Kalagasidis, A., Nielsen, T. R., Peuhkuri, R., and Hagentoft, C.-E. (2003). Presentation of the International Building Physics Toolbox for Simulink. *Proceedings of the 8th International Building performance Simulation (IBPSA) Conference*, Eindhoven, The Netherlands.

Wigbels, M., Bøhm, B. and Sipilae, K. (2005). Dynamic heat storage optimisation and demand side management. Annex VII I 2005:8DHC-05.06. IEA DHC/CHP

Appendix

Reference building and reference room

The plan of the reference building is inspired from a newly built existing detached single-family house. The total floor area is 105m². This building is broken up in seven rooms, see Figure A-1. The building is located in Göteborg at the south-west coast of Sweden, climate data with hourly resolution from the year of 1991 is applied in all simulation cases. The operation of the whole building is studied in Paper III. In Paper VI and VII is room 7 (12.6 m²) studied as a reference room. When only room 7 is considered the interior wall between zone 6 and 7 is modelled as an adiabatic wall with half the thickness. The considered building show small heat losses; the yearly space heating demand for the whole building is in the range of 25-30kWh/m²/year according to the simulations in Paper III. The space heating demand in room 7 is slightly higher since there are two windows and supply air in that particular room.

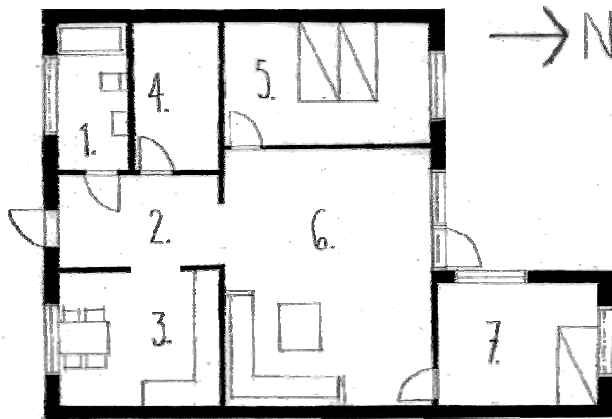


Figure A-1 Plan of the studied building.

Floor heating system

The reference building is fitted with a concrete embedded water-based floor heating system. Eight circuits cover the whole floor area. The outer pipe diameter is 16mm and the pipe wall is 2.2mm thick. Over the entire concrete slab, the centre-to-centre distance between the pipes is 300mm. The circuits are connected to a central manifold assembly and supplied with a common temperature. The centre of the pipe is mounted 20mm from the bottom of a 100mm thick concrete slab foundation. A 12mm wooden floor covers the top of the concrete slab. 250mm of thermal ground insulation is applied under the slab. Depending on the choice of surface heat transfer coefficient at the interior surface the insulation efficiency η for the floor heating system is in the range of 0.96-0.97. The total water flow rate is 0.338 l/s in the whole system. The reference room 7 is supplied with 0.05 l/s in a single pipe circuit.

Building envelope

All external walls are made of a conventional wooden frame structure with thermal insulation, which are covered with internal gypsum boards and external wooden cladding. The U-values for the different building components are given by Table A-1. All U-values includes the effect of thermal bridges in the thermal envelope. The entire thermal envelope including windows has an average U-value of $0.196 \text{ W/m}^2/\text{K}$. The average U-value for the thermal envelope in the reference room is $0.23 \text{ W/m}^2/\text{K}$.

Table A-1 U-values of the building and areas of building components in the reference room 7.

	U-value [W/m ² /K]	Area in room 7 [m ²]
Walls	0.20	23.0
Ceiling	0.12	12.6
Floor	0.10	12.6
Windows	1.1	4.32

Windows and shading

Energy efficient windows with triple glazing panes, inert gas and a low emission layer are used; the U-value is $1.1 \text{ W/m}^2/\text{K}$ for the entire window including thermal bridges. The simulation tool takes into account transmittance of solar heat through windows according to orientation, tilt and transmittance of the windowpanes. The climate file includes both direct and diffuse solar radiation with one-hour resolution. The terrain around the building is considered not causing any shading of the façade at any time of the year. In order to estimate a realistically influence from solar heat gains, the use of shading devices such as blinds or curtains is included; the shading coefficient is set to 0.48 for all windows. All interior materials have a solar absorptivity of 0.6.

Mechanical ventilation

The building is equipped with a balanced mechanical ventilation system with air-to-air heat recovery. The supply air flow rate is 40 l/s to the whole building. The heat recovery unit preheats the airflow before the supply air enters room 3, 5, 6 and 7. Exhaust air is taken from room 1, 3 and 4. The temperature efficiency of the heat recovery unit is 0.85. The supply airflow supplied to room 7 is 6.2 l/s.

Heat gains

A daily profile that takes into account daily variations in the use of household electricity is applied in order to estimate internal heat gains. Besides the daily profile, a yearly variation is also accounted for. The average supply of domestic electricity is 4.5 W/m^2 for the entire year. 70% of the electric energy is assumed to contribute to the heating of the building. The average heat supply from persons is estimated to 1.0 W/m^2 . All heat gains are assumed as purely convective in the analysis.